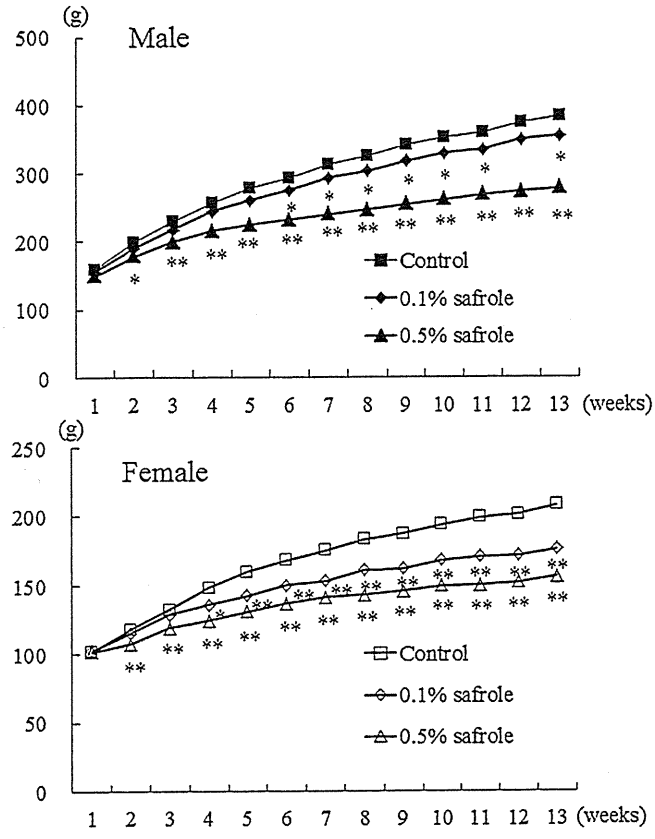

Fig. 1. Body weight curves for F344 *gpt* delta rats given safrole for 13 weeks. *,**: significantly different from the control group at $p < 0.05$ and $p < 0.01$, respectively.

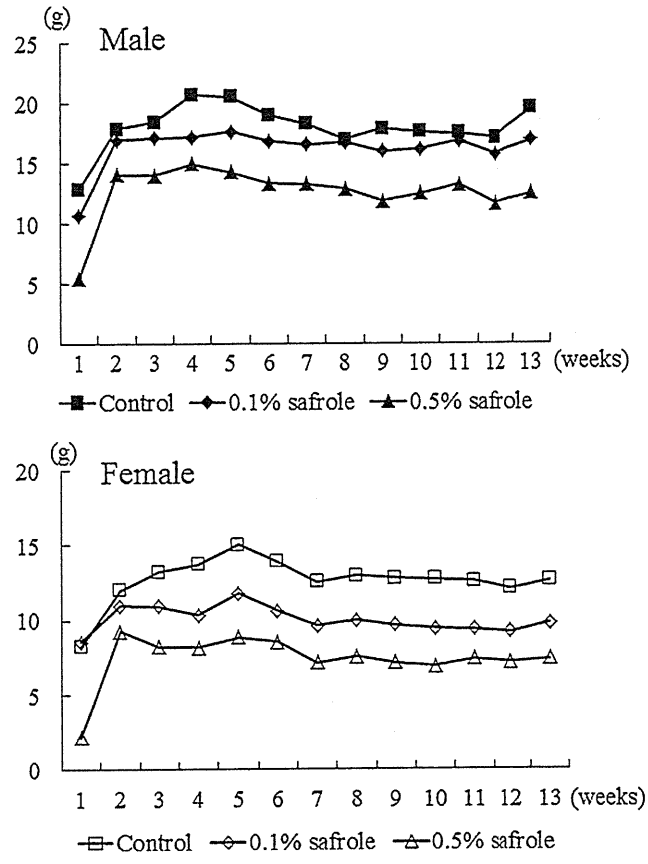

Fig. 2. Daily food intake for F344 *gpt* delta rats given safrole for 13 weeks. *,**: significantly different from the control group at $p < 0.05$ and $p < 0.01$, respectively.

Animals were given free access to a CRF-1 basal diet (Charles River Japan, Kanagawa, Japan) and tap water.

2.3. Experimental design

After a 1-week acclimatization period, animals were divided into 3 groups consisting of 10 male and 10 female F344 *gpt* delta rats per group, and given a diet containing 0.1%, 0.5% or 0% safrole for 13 weeks.

Clinical signs and general appearance were observed once a day. Body weight and food consumption were measured once a week. At the end of each period, the animals were euthanized under deep anesthesia. Left liver lobes were fixed with neutral-buffered formalin for histopathological and immunohistopathological examination. The remaining liver was stored at −80 °C for 8-OHdG measurements and *in vivo* mutation assays. At necropsy, blood samples were collected from the abdominal aorta for hematology and serum biochemistry. Relative organ weights were calculated as the values relative to body weights.

Hematological analysis was performed using an automated hematology analyzer, K-4500 (Sysmex Corp., Hyogo, Japan). Differential leukocyte and reticulocyte count were performed with a MICROX HEG-505 (Sysmex Corp.). Parameters for serum biochemistry shown in Table 3 were analyzed at SRL, Inc. (Tokyo, Japan) using sera frozen after centrifugation of whole blood.

At autopsy, weights of brain, heart, lungs, liver, kidneys, spleen, thymus, adrenal glands and testes were measured. In addition to these organs, the artery, bone/marrow, coagulation gland, esophagus, epididymides, large intestine (cecum, colon, and rectum), lymph node, mammary gland, pancreas, peripheral nerve, prostate gland, pituitary gland, thyroid glands, salivary gland, skeletal muscle, skin, small intestine (duodenum, jejunum, and ileum), spinal cord, stomach, urinary bladder, tongue, trachea, vagina, uterus, and ovaries were fixed in 10% neutral buffered formalin. Testes were fixed in Bouin's solution overnight and then transferred into 10% neutral buffered formalin. Tissues that needed decalcification, such as the nasal cavity, spinal cord with bones, sternum, and femur, were treated with a mixture of 10% formic acid and 10% neutral phosphate-buffered formalin. These tissues were routinely embedded in paraffin, sectioned at 3 μm thick for hematoxylin and eosin staining, and examined under light microscopy. Histopathological examinations were carried out for all groups.

2.4. In vivo mutation assays

The 6-TG and Spi⁻ (insensitive P2 interference) selection was carried out as previously described (Nohmi et al., 1996, 2000). Briefly, genomic DNA was extracted from liver tissue, and lambda EG10 DNA (48 kb) was rescued as the lambda phage through *in vitro* packaging. For 6-TG selection, the packaged phage was incubated with *E. coli* YG6020, expressing Cre recombinase, and converted to a plasmid carrying *gpt* and chloramphenicol acetyltransferase. Infected cells were mixed with molten soft agar and poured onto agar plates containing chloramphenicol and 6-TG. In order to determine the total number of rescued plasmids, infected cells were also poured on plates containing chloramphenicol without 6-TG. The plates were incubated at 37 °C for the selection of 6-TG resistant colonies, and the *gpt* mutant frequency (MF) was calculated by dividing the number of *gpt* mutants after clonal correction by the number of rescued phages. To characterize *gpt* mutations, a 739 bp DNA fragment containing the 456 bp coding region of the *gpt* gene was amplified by PCR as previously described, and the PCR products were analyzed with Applied Biosystems 3730 × 1 DNA Analyzer (Applied Biosystems Japan Ltd).

For Spi⁻ selection, the packaged phage was incubated with *E. coli* XL-1 Blue MRA for survival titration and *E. coli* XL-1 Blue MRA P2 for mutant selection. Infected cells were mixed with molten lambda-trypticase agar plates. The next day, plaques (Spi⁻ candidates) were punched out with sterilized glass pipettes and the agar plugs were suspended in SM buffer. In order to confirm the Spi⁻ phenotype of candidates, the suspensions were spotted on three types of plates containing XL-1 Blue MRA, XL-1 Blue MRA P2, or WL95 P2 strains and were spread with soft agar. The numbers of mutants that made clear plaques on each plate were counted as confirmed Spi⁻ mutants. The Spi⁻ MF was calculated by dividing the number of Spi⁻ mutants by the number of rescued phages. In all *in vivo* mutations assays, positive DNA samples were simultaneously applied to ensure the procedures well.

2.5. Measurement of nuclear 8-OHdG

In order to prevent 8-OHdG formation as a by-product during DNA isolation (Kasai, 2002), liver DNA was extracted using a slight modification of the method by Nakae et al. (1995). Briefly, nuclear DNA was extracted with a DNA Extractor WB Kit (Wako Pure Chemical Industries) containing an antioxidant NaI solution to dissolve cellular components. For further prevention of auto-oxidation in the cell lysis step, deferoxamine mesylate (Sigma Chemical, St. Louis, MO, USA) was added to the lysis buffer. The DNA was digested to deoxynucleotides by treatment with nuclease P1 and alkaline phosphatase and the levels of 8-OHdG (8-OHdG/10^5 dG) were measured by high-performance liquid chromatography with an electrochemical detection system (Coulochem II; ESA, Bedford, MA, USA).

Table 3
Serum biochemistry for F344 *gpt* delta rats given safrole for 13 weeks.

	Groups		
	Control	0.1% safrole	0.5% safrole
Males			
No. of animals examined	10	10	10
TP (g/dl)	7.0 ± 0.2[a]	7.0 ± 0.2	7.2 ± 0.2
A/G	2.0 ± 0.1	2.2 ± 0.1**	2.3 ± 0.1**
Alb (g/dl)	4.7 ± 0.1	4.8 ± 0.1	5.0 ± 0.2**
T-Bil (mg/dl)	0.04 ± 0	0.04 ± 0.01	0.03 ± 0.01**
Glucose (mg/dl)	159.3 ± 9.2	150.9 ± 7.2*	128.1 ± 3.9**
TG (mg/dl)	132.6 ± 61.8	83.3 ± 24.5	60.8 ± 23.7**
Phospholipid (mg/dl)	125.1 ± 16.7	117.4 ± 9.6	147.2 ± 12.5**
TC (mg/dl)	78.1 ± 6.5	76.3 ± 6.4	105.6 ± 9.8**
BUN (mg/dl)	19.3 ± 1.5	20.1 ± 0.7	23.6 ± 1.6**
CRN (mg/dl)	0.32 ± 0.01	0.34 ± 0.03	0.36 ± 0.03**
Na (mequiv./l)	145.9 ± 0.7	144.9 ± 0.7*	145.8 ± 1.1
Cl (mequiv./l)	106.1 ± 0.9	104.5 ± 1.2**	104.1 ± 1.3**
K (mequiv./l)	4.5 ± 0.2	4.4 ± 0.1	3.9 ± 0.9*
Ca (mg/dl)	10.8 ± 0.2	10.7 ± 0.2	11.2 ± 0.2**
IP (mg/dl)	5.7 ± 0.3	6.1 ± 0.5	6.0 ± 0.4
AST (IU/l)	98.9 ± 12.1	103.1 ± 7.0	117.4 ± 12.1**
ALT (IU/l)	54.1 ± 6.1	55.9 ± 4.8	102.7 ± 16.2**
ALP (IU/l)	497.3 ± 41.2	462.9 ± 49.1	375.0 ± 30.3**
Females			
No. of animals examined	9	10	10
TP (g/dl)	7.2 ± 0.3	6.6 ± 0.2**	6.9 ± 0.2*
A/G	2.7 ± 0.2	2.7 ± 0.1	2.6 ± 0.1
Alb (g/dl)	5.2 ± 0.2	4.9 ± 0.1**	5.0 ± 0.1*
T-Bil (mg/dl)	0.06 ± 0.01	0.05 ± 0.01*	0.04 ± 0.01**
Glucose (mg/dl)	130.6 ± 16.2	115.7 ± 11.1*	105.5 ± 10.4**
TG (mg/dl)	27.2 ± 7.5	15.3 ± 4.5**	25.3 ± 3.8
Phospholipid (mg/dl)	184.9 ± 19.5	164.8 ± 10.9*	247.9 ± 13.8**
TC (mg/dl)	108.2 ± 12.3	102.2 ± 6.9	186.0 ± 15.0**
BUN (mg/dl)	17.2 ± 2.7	17.9 ± 1.3	19.0 ± 2.0
CRN (mg/dl)	0.30 ± 0.03	0.31 ± 0.02	0.27 ± 0.02**
Na (mequiv./l)	144.1 ± 0.9	144.0 ± 1.3	143.4 ± 1.3
Cl (mequiv./l)	106.3 ± 1.9	107.0 ± 1.3	104.4 ± 1.5*
K (mequiv./l)	4.5 ± 1.7	4.0 ± 0.2	4.0 ± 0.2
Ca (mg/dl)	10.6 ± 0.5	10.3 ± 0.2	10.6 ± 0.1
IP (mg/dl)	6.7 ± 1.7	6.0 ± 0.6*	5.8 ± 0.3*
AST (IU/l)	82.7 ± 14.2	90.5 ± 5.1	115.1 ± 21.0**
ALT (IU/l)	42.6 ± 11.7	45.6 ± 3.7	61.7 ± 12.1**
ALP (IU/l)	343.6 ± 62.9	319.6 ± 33.4	350.9 ± 32.6

Abbreviations: TP, total protein; A/G, albumin/globulin ratio; Alb, albumin; T-Bil, total bilirubin; TG, triglyceride; TC, total cholesterol; BUN, blood urea nitrogen; CRN, creatinine; Na, sodium; Cl, chlorine; K, potassium; Ca, calcium; IP, inorganic phosphate; AST, aspartate aminotransferase; ALT, alanine aminotransferase; ALP, alkaline phosphatase.

[a] Mean ± SD.

* Significantly different from the controls at the levels of $p < 0.05$ (Dunnett's test).

** Significantly different from the controls at the levels of $p < 0.01$ (Dunnett's test).

2.6. Immunohistochemical staining for GST-P and proliferating cell nuclear antigen (PCNA)

Immunohistochemical staining was performed using polyclonal antibodies against GST-P (1:1000 dilution; Medical and Biological Laboratories Co., Ltd., Nagoya, Japan), a marker of preneoplastic lesions in the rat liver, and monoclonal anti-mouse PCNA antibodies (1:100; Dako, Glostrup, Denmark) to evaluate cell proliferation activity using the avidin–biotin peroxidase complex (ABC) method. The numbers (/cm^2) and areas (mm^2/cm^2) of the GST-P-positive foci (>0.1 mm^2) and the total areas of each liver section were measured using an IPAP image analyzer (Sumika Technos, Osaka, Japan) (Watanabe et al., 1994). The numbers of PCNA-positive cells per 600–800 intact liver cells from ten different areas per animal were counted to give the PCNA-positive ratio.

2.7. Statistics

The data obtained from the measurements of body weight, food and water consumption, organ weights, hematology, serum biochemistry, 8-OHdG levels, GST-P positive foci, PCNA-LI, *gpt* MFs and Spi$^-$ MFs were expressed as mean ± SD. The significant differences between the control and treated groups were determined by Dunnett's multiple comparison test (Dunnet, 1955) after ANOVA. The significant differences in incidences of lesions in the histopathological examinations were evaluated using Fisher's exact probability test. p-Values of less than 0.05 were considered statistically significant in both analyses.

3. Results

3.1. General condition, body weight, food consumption

One female from the control group died during the experimental period. However, no changes related to the death were observed in this rat. No remarkable changes in general appearances were observed in the safrole-treated groups during the experimental period. However, there was a marked suppression of body weight gain in the safrole-treated groups after week 2 (Fig. 1). Data for food consumption and safrole intake are summarized in Fig. 2 and Table 1. In both sexes, food consumption was decreased in the group given 0.5% safrole throughout the study, and the mean values for food consumption/animal were significantly lowered compared to the control group.

3.2. Hematology and serum biochemistry

The results of hematological measurements are shown in Table 2. White blood cell (WBC) counts and mean corpuscular hemoglobin (MCV) were significantly decreased and increased

Table 4
Organ weights in male F344 *gpt* delta rats given safrole for 13 weeks.

Groups No. of animal	Control 10	0.1% safrole 10	0.5% safrole 10
Body weight	369.5 ± 24.5[a]	341.1 ± 20.0**	264.4 ± 13.0**
Absolute (g)			
Liver	10.01 ± 0.80	9.90 ± 0.81	9.80 ± 0.86
Lungs	1.11 ± 0.07	1.06 ± 0.04	0.90 ± 0.06**
Kidneys	2.21 ± 0.13	2.14 ± 0.13	2.03 ± 0.12**
Brain	1.94 ± 0.07	2.00 ± 0.07	2.01 ± 0.35
Spleen	0.70 ± 0.05	0.66 ± 0.05	0.60 ± 0.05**
Thymus	0.24 ± 0.02	0.21 ± 0.02**	0.18 ± 0.02**
Heart	0.97 ± 0.06	0.88 ± 0.04**	0.72 ± 0.03**
Adrenals	0.045 ± 0.005	0.047 ± 0.004	0.048 ± 0.008
Testes	3.08 ± 0.16	3.10 ± 0.30	3.08 ± 0.14
Relative (g/100 g B.W.)			
Liver	2.71 ± 0.21	2.90 ± 0.15*	3.71 ± 0.37**
Lungs	0.30 ± 0.02	0.31 ± 0.01	0.34 ± 0.03**
Kidneys	0.60 ± 0.02	0.63 ± 0.03	0.77 ± 0.06**
Brain	0.53 ± 0.03	0.59 ± 0.02	0.76 ± 0.11**
Spleen	0.19 ± 0.01	0.19 ± 0.01	0.23 ± 0.02**
Thymus	0.07 ± 0.01	0.06 ± 0.01	0.07 ± 0.01
Heart	0.26 ± 0.01	0.26 ± 0.01	0.27 ± 0.02
Adrenals	0.012 ± 0.001	0.014 ± 0.001	0.017 ± 0.004**
Testes	0.84 ± 0.02	0.91 ± 0.06	1.17 ± 0.09**

[a] Mean ± SD.
* Significantly different from the controls at the levels of $p < 0.05$ (Dunnett's test).
** Significantly different from the controls at the levels of $p < 0.01$ (Dunnett's test).

respectively, in the treated groups of males. Conversely, significant increase of WBC counts was observed in the 0.5% group of females. In males, there was a significant decrease in red blood cell (RBC) counts and ratio of monocytes in the 0.5% group. In addition, significant increase of mean corpuscular hemoglobin (MCH) in the 0.5% group and decrease of platelet (Plt) counts in the 0.1% group were observed. In females, Plt counts and proportions of band form neutrophils, segmented neutrophils, eosinophils, reticulocytes showed significant decreases in the 0.5% group and proportions of lymphocytes showed significant increases in the treated group. In addition, a significant decrease of mean corpuscular volume (MCV) was observed in females of the 0.1% group.

Results from serum biochemical analysis are shown in Table 3. There were significant increases of aspartate (AST) and alanine aminotransferase (ALT) in both sexes in the 0.5% group. In males, significant increases of albumin (Alb), albumin/globulin (A/G) ratio, blood urea nitrogen (BUN), creatinine (CRN) and decreases of Glucose, triglyceride (TG), potassium (K), alkaline phosphatase (ALP) were observed in the 0.1% or 0.5% groups in a dose-dependent manner. In addition, significant increase of BUN, total cholesterol (TC) and calcium (Ca) and decrease of chlorine (Cl) were observed in males of the 0.5% group. In females, total protein (TP), albumin (Alb), total bilirubin (T-Bil), Glucose and inorganic phosphate (IP) were decreased in all treated groups. In addition, significant increase of TC and decrease of CRN and Cl were observed in the 0.5% group.

3.3. Organ weights and histopathological examination

Final body weights and the absolute and relative organ weights are shown in Tables 4 and 5. Final body weights were significantly decreased in the safrole-treated groups of both sexes. Absolute liver

Table 5
Organ weights in female F344 *gpt* delta rats given safrole for 13 weeks.

Groups No. of animal	Control 9	0.1% safrole 10	0.5% safrole 10
Body	202.1 ± 7.8[a]	168.7 ± 10.3**	150.1 ± 8.6**
Absolute (g)			
Liver	5.00 ± 0.42	4.62 ± 0.27**	5.65 ± 0.17**
Lungs	0.76 ± 0.03	0.73 ± 0.06	0.64 ± 0.04**
Kidneys	1.23 ± 0.06	1.13 ± 0.07*	1.09 ± 0.10**
Brain	1.82 ± 0.03	1.82 ± 0.08	1.76 ± 0.05
Spleen	0.43 ± 0.02	0.41 ± 0.02	0.40 ± 0.02**
Thymus	0.19 ± 0.01	0.18 ± 0.02	0.17 ± 0.02**
Heart	0.60 ± 0.02	0.53 ± 0.03**	0.45 ± 0.02**
Adrenals	0.052 ± 0.004	0.052 ± 0.005	0.046 ± 0.006**
Relative (g/100 g B.W.)			
Liver	2.48 ± 0.27	2.74 ± 0.10	3.77 ± 0.18**
Lungs	0.38 ± 0.03	0.44 ± 0.03**	0.43 ± 0.03**
Kidneys	0.61 ± 0.04	0.67 ± 0.02**	0.73 ± 0.04**
Brain	0.90 ± 0.04	1.08 ± 0.04**	1.17 ± 0.04**
Spleen	0.21 ± 0.01	0.25 ± 0.02**	0.26 ± 0.03**
Thymus	0.10 ± 0.01	0.11 ± 0.01	0.11 ± 0.02*
Heart	0.30 ± 0.02	0.31 ± 0.02	0.30 ± 0.01
Adrenals	0.026 ± 0.003	0.031 ± 0.002	0.030 ± 0.005

[a] Mean ± SD.
* Significantly different from the controls at the levels of $p < 0.05$ (Dunnett's test).
** Significantly different from the controls at the levels of $p < 0.01$ (Dunnett's test).

Table 6
Histopathological findings observed in F344 *gpt* delta rats given safrole for 13 weeks.

Organs	Findings	Sex	Male			Female		
		Groups	Control	0.1% safrole	0.5% safrole	Control	0.1% safrole	0.5% safrole
		No. of animals	10	10	10	9	10	10
Survival rate			100%	100%	100%	90%	100%	100%
Liver								
	Centrilobular vacuolar degeneration (large type)		1[a] (10[b])	6 (60)*	5 (50)	0 (0)	0 (0)	6 (60)**
	Single cell necrosis		1 (10)	9 (90)**	9 (90)**	4 (44)	7 (70)	6 (60)
	Centrilobular hepatocell hypertrophy		0 (0)	10 (100)**	10 (100)**	0 (0)	0 (00)	10 (100)**
	Microgranuloma		0 (0)	4 (40)*	2 (20)	0 (0)	1 (10)	2 (20)
Lung								
	Thrombus formation		3 (30)	1 (10)	1 (10)	0 (0)	0 (0)	1 (10)
	Focal hemorrhage		1 (10)	0 (0)	0 (0)	0 (0)	0 (0)	0 (0)
	Calcification		0 (0)	1 (10)	4 (40)*	0 (0)	0 (0)	0 (0)
	Foamy cell infiltration		0 (0)	1 (10)	1 (10)	1 (11)	1 (10)	1 (10)
	Inflammatory cell infiltration		0 (0)	0 (0)	1 (10)	0 (0)	0 (0)	0 (0)
	Arteritis		0 (0)	0 (0)	0 (0)	1 (11)	1 (10)	0 (0)
Kidney								
	Tubular hyaline droplets		0 (0)	0 (0)	10 (100)**	0 (0)	0 (0)	0 (0)
	Hyalin cast		0 (0)	2 (20)	3 (30)	0 (0)	0 (0)	0 (0)
	Tubular regeneration		1 (10)	9 (90)**	10 (100)**	0 (0)	0 (0)	0 (0)
	Granular cast		0 (0)	0 (0)	10 (100)**	0 (0)	0 (0)	0 (0)
	Pelvic calcification		0 (0)	0 (0)	10 (100)**	0 (0)	0 (0)	0 (0)
	Interstitial cell infiltration		0 (0)	0 (0)	6 (60)**	0 (0)	0 (0)	0 (0)
Heart								
	Myocardial inflammation		9 (90)	6 (60)	5 (50)	2 (22)	2 (20)	0 (0)
	Focal hemorrhage		0 (0)	1 (10)	0 (0)	0 (0)	0 (0)	0 (0)
Tongue								
	Inflammatory cell infiltration		1 (10)	2 (20)	3 (30)	0 (0)	1 (10)	0 (0)
Thyroid gland								
	Lymphoma		1 (10)	0 (0)	0 (0)	0 (0)	0 (0)	0 (0)
Parathyroid gland								
	Aberrant craniopharyngeal tissue		0 (0)	0 (0)	1 (10)	0 (0)	0 (0)	0 (0)
Pituitary gland								
	Anterior hyperplasia		0 (0)	0 (0)	0 (0)	0 (0)	0 (0)	1 (10)
Stomach								
	Inflammatory cell infiltration		1 (10)	0 (0)	0 (10)	0 (0)	0 (0)	0 (0)
Glandular stomach								
	Inflammatory cell infiltration		0 (0)	1 (10)	0 (0)	0 (0)	0 (0)	0 (0)
	Papilloma		0 (0)	0 (0)	0 (0)	0 (0)	1 (10)	0 (0)
Pancreas								
	Inflammatory cell infiltration		1 (10)	0 (0)	0 (0)	0 (0)	0 (0)	0 (0)
	Acinar atrophy		1 (10)	0 (0)	1 (10)	0 (0)	0 (0)	0 (0)
	Nesidioblastosis		0 (0)	0 (0)	0 (0)	0 (0)	1 (10)	0 (0)
Testis								
	Atrophy		0 (0)	1 (10)	0 (0)	–	–	–
Prostate gland								
	Prostatitis		0 (0)	1 (10)	0 (0)	–	–	–
Uterus								
	Extension		–	–	–	1 (11)	0 (0)	0 (0)
Deferent duct								
	Inflammatory cell infiltration		0 (0)	0 (0)	1 (10)	0 (0)	0 (0)	0 (0)
Bladder								
	Hydrops		0 (0)	0 (0)	1 (10)	0 (0)	0 (0)	0 (0)
Spinal cord cervical								
	Swelling of nerve cells		0 (0)	0 (0)	0 (0)	1 (11)	0 (0)	0 (0)

–, not examined.
[a] The number of animals with histopathological lesions.
[b] The incidence (%) of histopathological lesions.
* Significantly different from the controls at the levels of $p < 0.05$ (Dunnett's test).
** Significantly different from the controls at the levels of $p < 0.01$ (Dunnett's test).

weights in the 0.5% group of females and relative liver weights in the treated groups of males and in the 0.5% group of females significantly increased. In males, absolute weights of the lungs, kidneys, spleen, thymus and heart were statistically lower in the 0.5% group compared to the control group. In addition, a significantly decrease was observed in the thymus and heart of the 0.1% group as well. On the contrast, relative weights of the lungs, kidneys, brain, spleen, adrenals and testes were significantly increased in the 0.5% group compared to the control group. In females, significant decrease of the absolute weights of the lungs, spleen, thymus and adrenals were observed at the 0.5% group. But, the relative weights of these organs were significantly increased except for the adrenals. Furthermore, the absolute weights of the heart and kidneys were significantly decreased and relative weights of the brain and kidneys were significantly increased in the treated groups.

The results of histopathological examinations are shown in Table 6. Histopathologically, the incidence of centrilobular hypertrophy of hepatocytes was significantly increased in males of the treated groups and females in the 0.5% group compared with that in the control group (Fig. 3). Furthermore, in males, the single cell necrosis in the treated groups was significantly increased compared with that in the control group. The significant increase of centrilobular vacuolar degeneration was observed in males in the 0.1% group and in females in the 0.5% group. The incidences

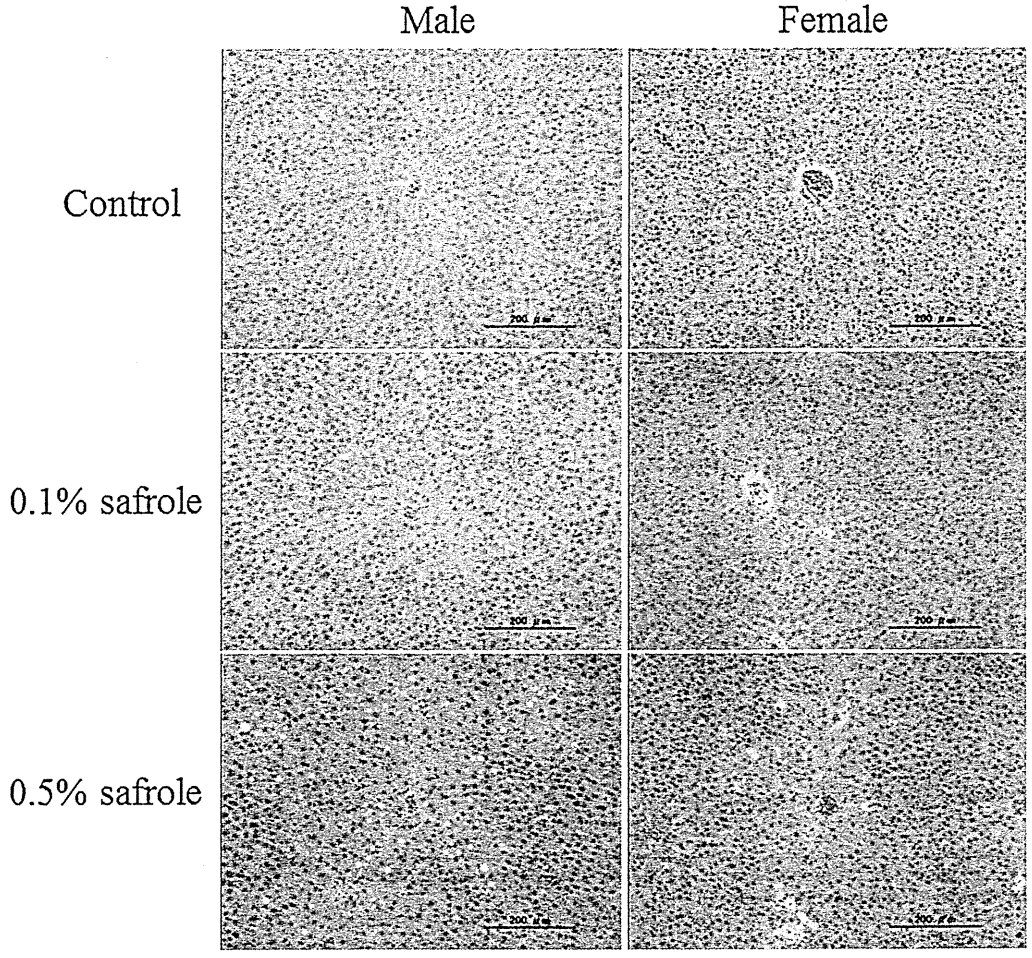

Fig. 3. Histopathological features in the livers of F344 *gpt* delta rats given safrole for 13 weeks. Centrilobular hypertrophy and vacuolar degeneration of hepatocytes are evident in the safrole-treated rats. HE stain. Bar represents 200 μm.

of tubular hyaline droplets, granular cast, pelvic calcification and interstitial cell infiltration of the kidney and of calcification of the lung were significantly increased in the males of the 0.5% groups. In addition, tubular regeneration of the kidney was significantly increased in the males of the all treated groups. On the other hand, thrombus formation and foamy cell infiltration of the lung, hyaline cast of the kidney, myocardial inflammation of the heart, and inflammatory cell infiltration of the tongue were observed in the treated rats without significant differences from the control group (10–60%).

3.4. *In vivo mutation assays in the livers*

Data for *gpt* and Spi$^-$ MFs in the liver of male and female *gpt* delta rats treated with safrole for 13 weeks are summarized in Tables 7 and 8, respectively. A significant increase of the *gpt* MFs was observed in males of the 0.5% (carcinogenic dose) group. In addition, increased *gpt* MFs were observed in females of the 0.5% group, although the increase was not statistically significant. There were no significant differences in the Spi$^-$ MFs among the groups in either sex. In the *gpt* mutant spectra, the predominant type of AT:GC transition was significantly induced by safrole (Table 9).

3.5. *Oxidative DNA damage in the liver*

In order to evaluate whether the oxidative damages to the cellular components occur during the formation of preneoplastic foci, the 8-OHdG levels were measured in liver DNA. The 8-OHdG levels in liver DNA were significantly increased in both sexes of the safrole-treated groups in a dose-dependent manner compared to those of the control groups (Table 10).

3.6. *Effects of safrole treatment on GST-P positive foci and cell proliferation*

Safrole treatment increased both the number and the area of GST-P positive foci in a dose-dependent manner compared with the control groups, although the differences were not statistically significant in males in the 0.1% group (Table 10). In addition, the effect of safrole on cell proliferation was evaluated by immunohistochemistry for PCNA (Table 10). The PCNA-positive ratio of hepatocytes was significantly increased in males of the treated groups and in females of the 0.5% group.

4. Discussion

A marked suppression of body weight gain was observed in the safrole-treated groups from week 2 to the end of the experiment. In serum biochemical examinations, there were significant increases of AST and ALT in both sexes of the 0.5% group. BUN and CRN levels significantly increased in males of the 0.5% group. In histopathological examinations, the incidences of centrilobular hypertrophy, centrilobular vacuolar degeneration and single cell necrosis of hepatocytes were significantly increased in males of the treated groups and in females of the 0.5% group. Furthermore, the incidences of tubular hyaline droplets, tubular regeneration, granular cast, pelvic

Table 7
gpt MFs in livers of F344 *gpt* delta rats given safrole for 13 weeks.

Sex	Groups	Animal no.	Cm^R colonies ($\times 10^5$)	6-TG^R and Cm^R colonies	Mutant frequency ($\times 10^{-5}$)	Mean ± S.D.
Male	Control	1	5.3	0	0.00	0.26 ± 0.21
		2	5.0	2	0.40	
		3	8.6	4	0.47	
		4	10.4	2	0.19	
		5	1.9	3	1.59[a]	
	0.1% safrole	11	6.3	4	0.63	0.77 ± 0.63
		12	4.5	8	1.76	
		13	5.3	5	0.95	
		14	4.7	1	0.21	
		15	7.2	2	0.28	
	0.5% safrole	21	3.4	7	2.05	1.89 ± 0.67**
		22	2.6	7	2.68	
		23	4.0	4	1.10	
		24	4.8	7	1.45	
		25	4.4	10	2.29	
Female	Control	36	6.9	7	1.01	0.65 ± 0.39
		37	4.9	3	0.62	
		38	5.1	0	0.00	
		39	7.7	7	0.90	
		40	5.6	4	0.71	
	0.1% safrole	46	6.2	9	1.46	0.98 ± 0.39
		47	7.6	10	1.32	
		48	12.8	10	0.78	
		49	5.3	3	0.57	
		50	7.9	6	0.76	
	0.5% safrole	56	2.8	3	1.06	1.26 ± 1.04
		57	3.3	3	0.91	
		58	3.6	2	0.56	
		59	3.2	10	3.09	
		60	3.0	2	0.66	

[a] Data of animal no. 5 was excluded for the calculation of the MF because of the poor packaging efficiency of the transgene (Smirnov–Grubbs test $T = 1.71$; $p < 0.05$).
** Significantly different from the control group at $p < 0.01$.

Table 8
Spi^- MFs in livers of F344 *gpt* delta rats given safrole for 13 weeks.

Sex	Groups	Animal no.	Plaques within XL-1 Blue MRA ($\times 10^5$)	Plaques within XL-1 Blue MRA (P2)	Mutant frequency ($\times 10^{-5}$)	Mean ± S.D.
Male	Control	1	9.5	9	0.94[a]	0.23 ± 0.51
		2	10.9	2	0.18	
		3	10.0	3	0.30	
		4	9.2	2	0.22	
		5	9.7	2	0.21	
	0.1% safrole	11	5.3	4	0.19	0.32 ± 0.25
		12	6.9	0	0.00	
		13	6.9	2	0.29	
		14	8.1	4	0.49	
		15	12.6	8	0.64	
	0.5% safrole	21	4.9	1	0.21	0.39 ± 0.29
		22	5.7	5	0.88	
		23	7.9	3	0.38	
		24	6.8	1	0.15	
		25	6.0	2	0.33	
Female	Control	36	7.1	1	0.14	0.36 ± 0.22
		37	6.7	3	0.45	
		38	9.8	1	0.10	
		39	8.3	4	0.48	
		40	11.5	7	0.61	
	0.1% safrole	46	6.9	0	0.00	0.21 ± 0.17
		47	7.4	1	0.14	
		48	11.4	5	0.44	
		49	7.1	1	0.14	
		50	9.5	3	0.31	
	0.5% safrole	56	2.5	2	0.79	0.29 ± 0.35
		57	5.3	0	0.00	
		58	6.0	1	0.17	
		59	6.0	3	0.50	
		60	8.7	0	0.00	

[a] Data of animal no. 1 was excluded for the calculation of the MF because of the poor packaging efficiency of the transgene (Smirnov–Grubbs test $T = 1.77$; $p < 0.05$).

Table 9
Mutation spectra of *gpt* mutant colonies in the livers of F344 *gpt* delta rats given safrole for 13 weeks.

Sex	Base substitution	Control		0.1% safrole		0.5% safrole	
		Number (%)	Mutation frequency (10^{-5})	Number (%)	Mutation frequency (10^{-5})	Number (%)	Mutation frequency (10^{-5})
Male	Transversions						
	GC-TA	2[a] (25.0)	0.06 ± 0.12	4(20.0)	0.15 ± 0.21	6(17.1)	0.30 ± 0.30
	GC-CG	1(12.5)	0.05 ± 0.09	2(10.0)	0.09 ± 0.20	4(11.4)	0.26 ± 0.31
	AT-TA	0	0	2(10.0)	0.07 ± 0.10	5(14.3)	0.29 ± 0.33
	AT-CG	0	0	0	0	1(2.9)	0.08 ± 0.17
	Transitions						
	GC-AT	4(50.0)	0.11 ± 0.12	8(40.0)	0.30 ± 0.25	5(14.3)	0.19 ± 0.18
	AT-GC	0	0	3(15.0)	0.12 ± 0.17	10(28.6)	0.54 ± 0.40**
	Deletion						
	Single bp	1(12.5)	0.05 ± 0.10	1(5.0)	0.04 ± 0.10	4(11.4)	0.19 ± 0.21
	Over 2 bp	0	0	0	0	0	0
	Insertion	0	0	0	0	0	0
	Complex	0	0	0	0	0	0
	Total	8	0.26 ± 0.21	20	0.77 ± 0.63	35	1.89 ± 0.67
Female	Transversions						
	GC-TA	4(19.0)	0.11 ± 0.19	10(26.3)	0.27 ± 0.17	5(25.0)	0.33 ± 0.45
	GC-CG	3(14.3)	0.08 ± 0.12	2(5.7)	0.04 ± 0.06	1(5.0)	0.06 ± 0.13
	AT-TA	1(4.8)	0.04 ± 0.09	6(15.8)	0.18 ± 0.19	2(10.0)	0.12 ± 0.28
	AT-CG	1(4.8)	0.04 ± 0.08	3(7.9)	0.08 ± 0.14	0	0
	Transitions						
	GC-AT	12(57.1)	0.38 ± 0.22	8(21.1)	0.18 ± 0.15	6(15.0)	0.37 ± 0.34
	AT-GC	0	0	8(21.1)	0.21 ± 0.05	5(25.0)	0.31 ± 0.31
	Deletion						
	Single bp	0	0	1(2.6)	0.03 ± 0.06	1(5.0)	0.07 ± 0.15
	Over 2 bp	0	0	0	0	0	0
	Insertion	0	0	0	0	0	0
	Complex	0	0	0	0	0	0
	Total	21	0.65 ± 0.39	38	0.98 ± 0.39	20	1.26 ± 1.04

[a] Number of colonies with independent mutations.
** Significantly different from the control group at $p < 0.01$.

calcification and interstitial cell infiltration in the kidney were significantly increased in males of the treated groups. The overall data indicated that safrole is a nephrotoxicant as well as a hepatotoxicant. In previous studies, the suppression of body weight gain and liver enlargement were also observed in safrole-treated rats (Homburger et al., 1962; Hagan et al., 1965). These results show that the *gpt* delta rat has a similar sensitivity to safrole in comparison to non-transgenic wild rats. This implies that the *gpt* delta rat model can be used to investigate general toxicities of agents.

Safrole forms safrole-specific DNA adducts through hepatic cytochrome P450 biotransformation and subsequent conjugation by sulfotransferase (Miller and Miller, 1983). Alternatively, safrole can be biotransformed though the methylenedioxy ring-opening to hydroxychavicol. Hydroxychavicol could be biotransformed to o-quinone through 2-electron oxidation, and this redox-active quinone is considered to induce oxidative damages (Klungsoyr and Scheline, 1983; O'Brien, 1991). In fact, the levels of 8-OHdG were significantly increased in both sexes of the safrole-treated groups as compared to those of the control group. To the best of our knowledge, there are no reports demonstrating the significant increase of 8-OHdG levels in livers of rats treated with a low dose (half of a carcinogenic dose) for 13 weeks. However, the genotoxicity of safrole remained unknown in conventional genotoxicity tests such as the Ames test, sister chromatid exchanges (SCE) test and micronucleus test in spite of its hepatocarcinogenicity being clear (Green and Savage, 1978; Swanson et al., 1979; Baker and Bonin, 1985; Bradley, 1985; Gocke et al., 1981). The present study demonstrated that an increase or increasing tendency of the *gpt* MFs was observed in both sexes in the 0.5% group, a carcinogenic dose, despite the Spi^- MFs being unchanged. These results suggested that safrole has a potential to be genotoxic *in vivo* in the livers of rats. In the mutation spectra, the AT:GC transitions were significantly induced by safrole in males of the 0.5% group. If has been reported that 8-OHdG is capable to form a base pair with adenine and subsequently produce a GC:AT transversion mutation. In addition, recent studies suggest that 8-OHdG can cause large deletion mutations associated with double strand break during base excision repair by *OGG1* (Umemura

Table 10
8-OHdG, PCNA and GST-P levels in the livers of F344 *gpt* delta rats given safrole for 13 weeks.

Sex	Treatment	Control	0.1% safrole	0.5% safrole
Male	8-OHdG	0.27 ± 0.02[a]	0.35 ± 0.05*	0.52 ± 0.06**
	PCNA-positive ratio	0.27 ± 0.12	0.54 ± 0.17*	0.51 ± 0.14*
	GST-P (number/cm^2)	0.00 ± 0.00	0.88 ± 0.55	9.42 ± 3.51**
	GST-P (mm^2/cm^2)	0.00 ± 0.00	0.005 ± 0.004	0.134 ± 0.070**
Female	8-OHdG	0.36 ± 0.04	0.51 ± 0.06**	0.62 ± 0.06**
	PCNA-positive ratio	0.20 ± 0.07	0.66 ± 0.09	1.06 ± 0.55**
	GST-P (number/cm^2)	0.00 ± 0.00	0.44 ± 0.46*	2.78 ± 1.22**
	GST-P (mm^2/cm^2)	0.00 ± 0.00	0.004 ± 0.005	0.026 ± 0.016**

[a] Mean ± SD.
* Significantly different from the controls at the levels of $p < 0.05$ (Dunnett's test).
** Significantly different from the controls at the levels of $p < 0.01$ (Dunnett's test).

et al., 2007). Thus, in the light of the type of mutations induced by safrole, it is unlikely that 8-OHdG formation contributes to safrole-induced genotoxicity, although there is a possibility of any other oxidized DNA damages being involved. The present data showing a significant increase in PCNA-positive hepatocytes might suggest the possible participation of oxidative stress in cell proliferation.

It is well known that the results of bioassay using GST-P-positive foci show good correlation with those of the 2-year cancer bioassay (Ito et al., 2000; Ogiso et al., 1985). Therefore, it has been widely accepted that the analysis of GST-P positive foci may be a useful indicator to predict carcinogenicity of agents. In the present study, the number and the area of GST-P positive foci were significantly increased in both sexes in the 0.5% group. The data on quantitative analysis for GST-P foci using *gpt* delta rats are also in agreement with the carcinogenicity data previously reported by Long et al. (1963).

In conclusion, the present medium-term animal model using F344 *gpt* delta rats confirmed previous reports of the hepatotoxicity and hepatocarcinogenicity of safrole. The genotoxicity of safrole, which remained unknown, so far, was clearly demonstrated in the target organ by this *in vivo* model. Thus, this animal model might be a promising tool for investigating comprehensive toxicities of agents. The acquisition of additional data on key events in chemical carcinogenesis, such as base modification and cell proliferation, could assist in understanding the modes of action. Applications of this model should be further expanded in future studies.

Conflict of interest statement

None.

Acknowledgements

We thank Ms. Ayako Kaneko and Ms. Yoshimi Komatsu for their expert technical assistance. This work was supported by a Grant-in-Aid for Research on Food Sanitation from the Ministry of Health, Labor and Welfare of Japan (H21-shokuhin-ippan-010).

References

Baker, R.S.U., Bonin, A.M., 1985. Tests with *Salmonella* plate incorporation assay. In: Ashby, J., De Serres, F.J. (Eds.), Evaluation of Short-term Tests for Carcinogens. Elsevier, NY, pp. 177–180.

Borchert, P., Wislocki, P.G., Miller, J.A., Miller, E.C., 1973. The metabolism of the naturally occurring hepatocarcinogen safrole to 1′-hydroxysafrole and the electrophilic reactivity of 1′-acetoxysafrole. Cancer Res. 33, 575–589.

Bradley, M.O., 1985. Measurement of DNA single-strand breaks by alkaline elution in rat hepatocytes. In: Ashby, J., De Serres, F.J. (Eds.), Evaluation of Short-term Tests for Carcinogens. Elsevier, NY, pp. 353–357.

Daimon, H., Sawada, S., Asakura, S., Sagami, F., 1998. In vivo genotoxicity and DNA adduct levels in the liver of rats treated with safrole. Carcinogenesis 19, 141–146.

Dorange, J.L., Janiaud, P., Delaforge, M., et al., 1978. Comparative survey of microsomal activation system for mutagenic studies of safrole. Mutat. Res. 52, 179–180.

Dunnet, C.W., 1955. A multiple comparison procedure for comparing several treatments with a control. Am. Stat. Assoc. J. 50, 1096–1121.

Furia, T.E., Bellanca, N., 1975. Fenaroli's Handbook of Flavor Ingredients, vol. 2., 2nd ed. CRC press, Cleveland, OH.

Gocke, E., King, M.T., Eckardt, K., Wild, D., 1981. Mutagenicity of cosmetics ingredients licensed by the European Community. Mutat. Res. 90, 91–109.

Green, N.R., Savage, J.R., 1978. Screening of safrole, eugenol, their ninhydrin positive metabolites and selected secondary amines for potential mutagenicity. Mutat. Res. 57, 115–121.

Hagan, E.C., Jenner, P.M., Jones, W.I., et al., 1965. Toxic properties of compounds related to safrole. Toxicol. Appl. Pharmacol. 7, 18–24.

Hayashi, H., Kondo, H., Masumura, K., et al., 2003. Novel transgenic rat for *in vivo* genotoxicity assays using 6-thioguanine and Spi$^-$ selection. Environ. Mol. Mutagen. 41, 253–259.

Homburger, F., Kelley Jr., T., Baker, T.R., Russfield, A.B., 1962. Sex effect on hepatic pathology from deficient diet and safrole in rats. Arch. Pathol. 73, 118–125.

IARC, 1976. Monographs on the Evaluation of Carcinogenic Risk of Chemicals to Man. Safrole, Isosafrole and Dihydrosafrole, vol. 10. International Agency for Research on Cancer, Lyon, France, pp. 231–244.

Ioannides, C., Delaforge, M., Parke, D.V., 1981. Safrole: its metabolism, carcinogenicity and interactions with cytochrome P450. Food Cosmet. Toxicol. 19, 657–666.

Ito, N., Imaida, K., Asamoto, M., Shirai, T., 2000. Early detection of carcinogenic substances and modifiers in rats. Mutat. Res. 462, 209–217.

Kasai, H., 2002. Chemistry-based studies on oxidative DNA damage: formation, repair, and mutagenesis. Free Radic. Biol. Med. 33, 450–456.

Klungsoyr, J., Scheline, R.R., 1983. Metabolism of safrole in the rat. Acta Pharmacol. Toxicol. 52, 211–216.

Leung, A.Y., 1980. Encyclopedia of Common Natural Ingredients Used in Food, Drugs, and Cosmetics. John Wiley, New York.

Liu, T.Y., Chen, C.C., Chen, C.L., Chi, C.W., 1999. Safrole-induced oxidative damage in the liver of Sprague-Dawley rats. Food Chem. Toxicol. 37, 697–702.

Long, E.L., et al., 1963. Liver tumors produced in rats by feeding safrole. Arch. Pathol. 75, 595–604.

Masumura, K., Horiguchi, M., Nishikawa, A., et al., 2003. Low dose genotoxicity of 2-amino-3,8-dimethylimidazo[4,5-*f*]quinolone (MeIQx) in *gpt* delta transgenic mice. Mutat. Res. 541, 91–102.

Miller, J.A., Miller, E.C., 1983. The metabolic activation and nucleic acid adducts of naturally-occurring carcinogens. Recent results with ethyl carbamate and the spice flavors safrole and estragole. Br. J. Cancer 48, 1–15.

Nakae, D., Mizumoto, Y., Kobayashi, E., et al., 1995. Improved fenomic/nuclear DNA extraction for 8-hydroxydeoxyguanosine analysis of small amounts of rat liver tissue. Cancer Lett. 97, 233–239.

Natarajan, A.T., Darroudi, F., 1991. Use of human hepatoma cells for *in vitro* metabolic activation of chemical mutagens/carcinogens. Mutagenesis 6, 399–403.

Nohmi, T., Katoh, M., Suzuki, H., et al., 1996. A new transgenic mouse mutagenesis test system using Spi$^-$ and 6-thioguanine selections. Environ. Mol. Mutagen. 28, 465–470.

Nohmi, T., Suzuki, K., Masumura, M., 2000. Recent advances in the protocols of transgenic mouse mutation assays. Mutat. Res. 455, 191–215.

O'Brien, P.J., 1991. Molecular mechanisms of quinine cytotoxicity. Chem. Biol. Interact. 80, 1–11.

Ogiso, T., Tatematsu, M., Tamano, S., et al., 1985. Comparative effects of carcinogens on the induction of placental glutathione S-transferase-positive liver nodules in a short-term assay and of hepatocellular carcinomas in a long-term assay. Toxicol. Pathol. 13, 257–265.

Swanson, A.B., Chambliss, D.D., Blanquist, J.C., et al., 1979. The mutagenicities of safrole, estragole, trans-anethole and some of their known or possible metabolites for *Salmonella thyphimurium* mutants. Mutat. Res. 60, 143–153.

To, L.P., Hunt, T.P., Andersen, M.E., 1982. Mutagenicity of trans-anethole, estragole, eugenol, and safrole in the Ames *Salmonella typhimurium* assay. Bull. Environ. Contam. Toxicol. 28, 647–654.

Toyoda-Hokaiwado, N., Inoue, T., Masumura, K., et al., 2010. Integration of *in vivo* genotoxicity and short-term carcinogenicity assays using F344 *gpt* delta transgenic rats: *in vivo* mutagenicity of 2,4-diaminotoluene and 2,6-diaminotoluene structural isomers. Toxicol. Sci. 114, 71–78.

Umemura, T., Kuroiwa, Y., Tasaki, M., et al., 2007. Detection of oxidative DNA damage, cell proliferation and *in vivo* mutagenicity induced by dicyclanil, a non-genotoxic carcinogen, using *gpt* delta mice. Mutat. Res. 633, 46–54.

Umemura, T., Tasaki, M., Kijima, A., et al., 2009. Possible participation of oxidative stress in causation of cell proliferation and *in vivo* mutagenicity in kidneys of *gpt* delta rats treated with potassium bromate. Toxicology 257, 46–52.

Watanabe, T., Katsura, Y., Yoshitake, A., et al., 1994. IPAP: image processor for analytical pathology. J. Toxicol. Pathol. 7, 353–361.

Wislocki, P.G., Miller, E.C., Miller, J.A., et al., 1977. Carcinogenic and mutagenic activities of safrole. 1′-Hydroxysafrole, and same known or possible metabolites. Cancer Res. 37, 1883–1891.

Chemical Research in Toxicology

ARTICLE

pubs.acs.org/crt

Detection and Quantification of Specific DNA Adducts by Liquid Chromatography−Tandem Mass Spectrometry in the Livers of Rats Given Estragole at the Carcinogenic Dose

Yuji Ishii,*,† Yuta Suzuki,† Daisuke Hibi,† Meilan Jin,† Kiyoshi Fukuhara,‡ Takashi Umemura,† and Akiyoshi Nishikawa†

†Division of Pathology and ‡Division of Organic Chemistry, National Institute of Health Sciences, 1-18-1 Kamiyoga, Setagaya-ku, Tokyo 158-8501, Japan

ABSTRACT: Estragole (ES) is a natural constituent of several herbs and spices that acts as a carcinogen in the livers of rodents. Given that the proximal electrophilic form of ES with a reactive carbocation is generated by cytochrome P450 and a sulfotransferase metabolizing pathway, there is a possibility that the resultant covalent adducts with DNA bases may play a key role in carcinogenesis. The existence of ES-specific deoxyguanosine (dG) and deoxyadenosine (dA) adducts has already been reported with the precise chemical structures of the dG adducts being confirmed. In the present study, we examined ES-specific dA adduct formation using LC-ESI/MS after the reaction of dA with 1′-acetoxy-ES produced by a sulfotransferase metabolic pathway mimic. Although two peaks were observed in the LC-ESI/MS chromatogram, the identification of ES-3′-N^6-dA as the measurable peak was determined by NMR analysis. To confirm ES-specific dG and dA adduct formation in vivo, an isotope dilution LC-ESI/MS/MS method applicable to in vivo samples for ES-3′-N^6-dA together with the two major dG adducts, that is, ES-3′-C8-dG and ES-3′-N^2-dG, was developed using selected ion recording. The limit of quantification was 0.2 fmol on column for ES-3′-C8-dG and ES-3′-N^2-dG and 0.06 fmol on column for ES-3′-N^6-dA, respectively. Using the developing analytical method, we attempted to measure adduct levels in the livers of rats treated with ES at a possible carcinogenic dose (600 mg/kg bw) for 4 weeks. ES-3′-C8-dG, ES-N^2-dG, and ES-3′-N^6-dA were detected at levels of 3.5 ± 0.4, 4.8 ± 0.8, and 20.5 ± 1.6/10^6 dG or dA in the livers of ES-treated rats. This quantitative data and newly developed technique for adduct observation in vivo might be helpful for ES hepatocarcinogenesis investigations.

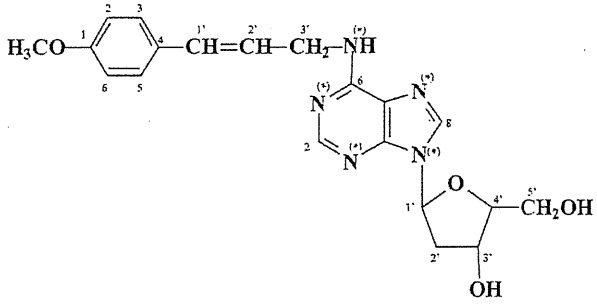

INTRODUCTION

Estragole (4-allyl-1-methoxybenzene; ES) is a natural constituent of essential oils of various herbs and spices (including tarragon, basil, fennel, and anise) present in food.[1] Previous studies have revealed that ES has genotoxicity and carcinogenicity in the livers of mice, concluding that ES is a naturally occurring genotoxic carcinogen.[2−4] ES is metabolized to the proximate carcinogen, 1′-hydroxy-ES, by cytochrome P450 enzymes (P450), and sulfotransferase (SULT) converts 1′-hydroxy-ES to 1′-sulfooxy-ES.[2−5] The ultimate electrophilic carbocation structure, which can form covalent adducts with DNA bases, is formed from 1-sulfooxy-ES through dissociation of the sulfate group.[6,7] Because postlabeling analysis demonstrated the formation of four different adducts such as ES-3′-N^2-dG (deoxyguanosine), ES-3′-C8-dG, ES-1′-N^2-dG, and ES-3′-N^6-dA (deoxyadenosine) in the livers of mice administered the proximate carcinogenic metabolite 1′-hydroxy-ES, it has been accepted that the carcinogenicity of ES is caused by the formation of these adducts.[8−11] However, the precise amount of these adducts formed in vivo under continuous administration with a carcinogenic dose of ES still remains unknown. Transient base modifications of DNA do not always result in gene mutations because of chemical DNA instability[12] and the existence of specific DNA repair systems.[13] Because the specific activity of repair enzymes is primarily dependent on stereochemical structures and concentrations of their substrates, confirmation of DNA base modifications and precise quantification are necessary for understanding their biological significance.[14,15]

The dG modifications have generally been reported as the major adduct,[16,17] because dG is the most potent nucleophilic nucleoside that can efficiently react with the electrophilic carbocation form.[18] Furthermore, the findings of Y-family polymerase κ, which selectively acts on translesion synthesis on N^2-dG adducts, showed the presence of a linkage between dG modification and mutation in the chemical carcinogenicity.[19−21] However, several carcinogens including aristolochic acid[22,23] and polyaromatic hydrocarbons[24] preferentially form dA adducts,

Received: November 27, 2010
Published: March 08, 2011

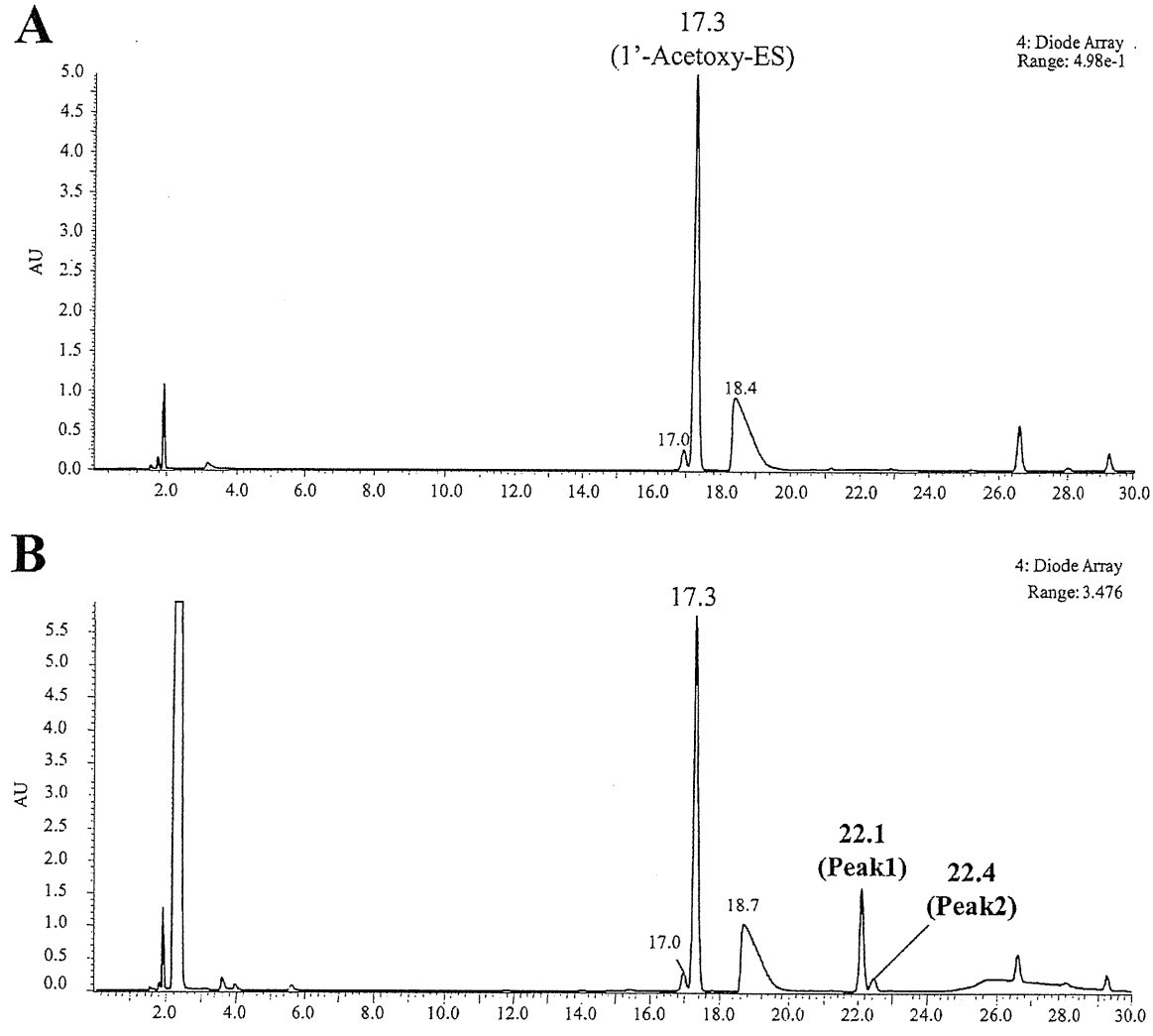

Figure 1. Typical LC-PDA chromatograms (280 nm) in the reaction of (A) 1′-acetoxy-ES alone and (B) 1′-acetoxy-ES with dA. LC-PDA conditions are described in the Materials and Methods.

thereby predominantly inducing dA mutations.[25,26] Thus, quantitative analysis for each ES-modified base is necessary to investigate the role of specific DNA adducts in ES carcinogenesis.

Although the exact chemical structure of three dG adducts has already been confirmed by mass spectrometry (MS) techniques, that of the dA adduct has not been identified. In this study, ES-dA adduct formation by reaction of dA with 1′-acetoxy-ES (used as a 1′-sulfooxy-ES mimic) was investigated by liquid chromatography (LC)-electron spray ionization (ESI)/MS analysis. The precise chemical structures of the detected adducts were identified using nuclear magnetic resonance (NMR). Subsequently, a quantitative analytical method using LC-ESI/tandem mass spectrometry (MS/MS) for ES-specific dG and dA adducts was developed. After the evaluation of applicability to in vivo samples, our LC-ESI/MS/MS method was applied to quantify ES-specific DNA adducts in the livers of rats treated with 600 mg/kg bw of ES for 4 weeks.

MATERIALS AND METHODS

Chemicals and Reagents. ES, *p*-anisaldehyde, vinylmagnesium bromide, tetrahydrofuran (THF), dG, dA, and alkaline phosphatase were purchased from Sigma Chemical Co. (St. Louis, MO). Nuclease P1 was from Yamasa Shoyu Co. (Chiba, Japan). Stable isotope-labeled [$^{15}N_5$]-dG and [$^{15}N_5$]-dA were obtained from Cambridge Isotope Laboratories (Cambridge, MA). Acetic anhydride ammonium carbonate, dimethylsulfoxide (DMSO), dichloromethane, *N*,*N*-dimethylformamide (DMF), diethyl ether, isopropyl alcohol, and DNA extractor TIS kit were purchased from Wako Pure Chemicals (Tokyo, Japan). All other chemicals used were of specific analytical or HPLC grade.

Synthesis of 1′-Hydroxyestragole. 1′-Hydroxy-ES was synthesized from *p*-anisaldehyde as described by Punt et al.[7] The synthesis of 1′-hydroxy-ES encompassed a Grignard reaction, using vinylmagnesium bromide as the Grignard reagent (1 M solution in THF). Briefly, *p*-anisaldehyde (0.0165 mol) was dissolved in 10 mL of dry THF, and this solution was added dropwise over a period of 30 min to the Grignard reagent (0.035 mol) while stirring at 50 °C in anhydrous conditions under a nitrogen atmosphere. The reaction mixture was further incubated for 90 min, and the resulting solution was added to a solution of 4.5 g of ammonium chloride in 200 mL of ice cold water. The emulsion was stirred for several minutes, and 1′-hydroxy-ES was extracted with diethyl ether. The organic solution was dried with magnesium sulfate, and the yield was 94%. The identity of the product was confirmed by ^{1}H NMR. ^{1}H NMR spectra were recorded with a Varian 500 MHz NMR system

dx.doi.org/10.1021/tx100410y |*Chem. Res. Toxicol.* 2011, 24, 532–541

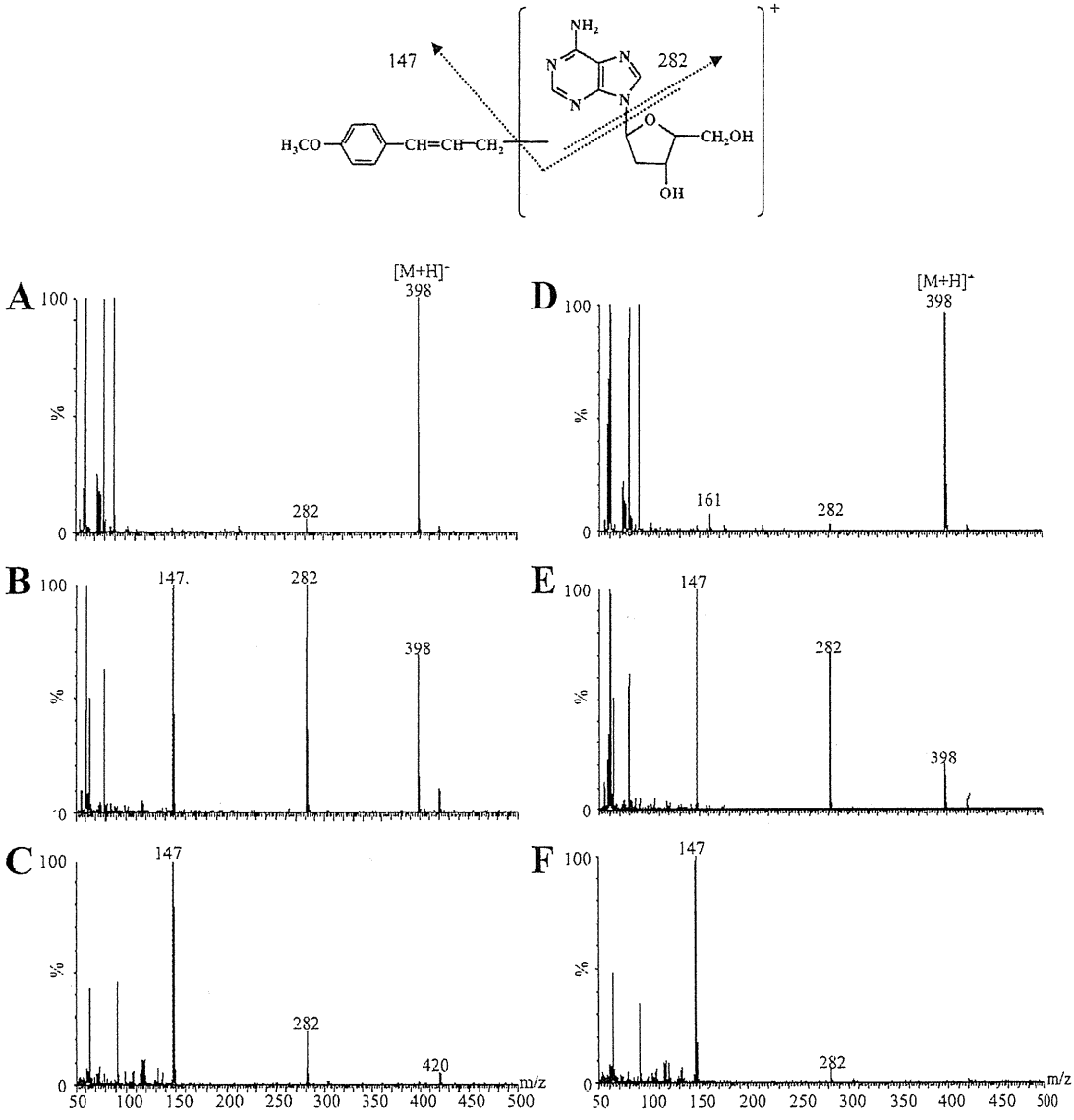

Figure 2. Mass spectra of peaks 1 (A–C) and 2 (D–F) obtained from LC-ESI/MS analysis for the reaction of 1′-acetoxy-ES with dA. Mass analysis was performed in scan mode. The cone voltages were 20 (A and D), 40 (B and E), and 60 V (C and E) in positive ion mode. LC-ESI/MS conditions are described in the Materials and Methods.

(Varian Inc. Corp.). 1′-Hydroxy-ES: ^{1}H NMR (DMSO-d_6): δ 7.22–7.29 (m, 2H, Ar), 6.82–6.89 (m, 2H, Ar), 5.98–6.10 (m, 1H, $-CHCH_2$), 5.26–5.35 [m, 2H, $-C(OH)CH-$], 5.10–5.20 (m, 2H, $-CHCH_2$), 3.79 (s, 1H, $-OCH_3$), 2.24 [s, 1H, $-C(OH)-$].

Synthesis of 1′-Acetoxyestragole. 1′-Acetoxy-ES was synthesized from 1′-hydroxy-ES as described by Punt et al.[7] and Drinkwater et al.[2] In brief, 1′-hydroxy-ES (50 mg) was dissolved in 200 μL of pyridine. Acetic anhydride (33 μL) was added dropwise to this solution, and the reaction mixture was stirred for 5 h at room temperature after which 400 μL of dichloromethane was added. The reaction mixture was extracted several times with aliquots of 200 μL of 1 N HCl. When the aqueous phase reached pH 2–3, the organic layer then immediately was extracted with 400 μL of 1 M sodium carbonate solution (pH 7.6). The organic solution was dried with magnesium sulfate, and the solvent was evaporated in a nitrogen atmosphere. The identity of the product was confirmed by ^{1}H NMR. 1′-Hydroxy-ES: ^{1}H NMR (DMSO-d_6): δ 7.26–7.28 (m, 2H, Ar), 6.92–6.95 (m, 2H, Ar), 5.99–6.07 (m, 1H, $-CHCH_2$), 5.26–5.27 [m, 2H, $-CH(OH)CH-$], 5.19–5.23 (m, 2H, $-CHCH_2$), 3.75 (s, 1H, $-OCH_3$), 2.05 (s, 1H, $-CO-CH_3$).

Determination of ES-Specific dA Adduct. ES-specific dA adducts were determined from reactions between 1′-acetoxy-ES and dA based on the protocol of Phillips et al.[8] The reaction products containing 1′-acetoxy-ES were diluted 50-fold in DMF from which 200 μL was added to 1.8 mL of 10 mM dA solution in 50 mM sodium phosphate buffer (pH 7.4). The reaction mixture was stirred for 24 h at 37 °C. The reaction mixture was then passed through an HLC-DISK syringe filter (Kanto Chemical Co Inc., Tokyo) and was separated on a LC-photodiode array (PDA)-ESI/MS system. LC-PDA-ESI/MS analyses were performed using an Alliance HT model 2695 liquid chromatographic system coupled to a 996 PDA detector and Micromass ZQ, a single quadrupole, MS system (Waters Corp., Miliford, MA) equipped with an ESI source through a splitter. Twenty microliters of the reaction mixture was injected directly onto a reverse-phase C_{18} column (Mightysil RP-18, 4.6 mm × 150 mm, 5 μm, Kanto Chemical Co.,

Table 1. ^{1}H NMR Chemical Shifts of Peak 1[a]

H-1′	6.34 (1H, m)
H-2′	2.70 (1H, m)
H-2″	2.25 (1H, m)
H-3′	4.40 (1H, m)
H-4′	3.87 (1H, m)
H-5′	3.61 (1H, m)
H-5″	3.51 (1H, m)
OH-3′	5.31 (1H, s)
OH-5′	5.22 (lH,bs)
H-2	8.21 (1H, bs)
H-8	8.37 (1H, s)
N^6-H	8.07 (lH,bs)
ESH-1′	6.42 (1H, m)
ESH-2′	6.21 (1H, m)
ESH-3′	4.22 (2H, bs)
ESH-2,6	7.30 (2H, m)
ESH-3,5	6.85 (2H, m)
$ESOCH_3$	3.75 (3H, m)

[a] m, multiplet; s, singlet.

Inc.) maintained at 40 °C. Solvent A was water, solvent B was methanol, and solvent C was 0.1% formic acid. The column was equilibrated with a mixture of solvent A/solvent B/solvent C (70/10/20, v/v). A linear gradient was applied from 30 to 90% methanol over 40 min, kept at 90% for 10 min, lowered to 20% over 2 min, and re-equilibrated at the initial conditions for 15 min. Mass analysis was performed in scan mode. The cone voltages were 20, 40, and 60 V in the positive ion mode.

Synthesis of ES-Derived dA Adduct. ES-dA adducts were synthesized from a reaction between 1′-acetoxy-ES and dA. Four milliliters of 30 mM 1′-acetoxy-ES solution in dichloromethane was diluted 50-fold in DMF from which 200 mL was added to 1800 mL of 10 mM dG or dA solution in 50 mM sodium phosphate buffer (pH 7.4). The reaction was stirred for 24 h at 50 °C. The yield of peak 1 was 86 mg (7.1%). The reaction was repeated several times as needed to acquire enough products for NMR analysis.

Purification was performed using the combined reaction mixtures that were evaporated and reconstituted in 50% methanol/water. The concentrated reaction mixture was separated by a LC system equipped with a UV detector (LC-UV) (PU-2080 Plus Intelligent HPLC Pump, AS-2057 plus Intelligent Sampler, CO-966 Intelligent Column Thermostat, and UV-970 Intelligent UV/vis Detector; Jasco Co., Tokyo). Two milliliters of sample was injected directly on to a reverse phase C_{18} column (Mightysil RP-18 GP, 20 mm × 250 mm, 5 μm, Kanto Chemical Co., Inc.) maintained at 40 °C. Solvent A was 0.01% formic acid, and solvent B was methanol containing 0.01% formic acid. The column was equilibrated with a mixture of solvent A/solvent B (70/30, v/v). A linear gradient was applied from 30 to 90% methanol over 30 min, kept at 90% for 10 min, lowered to 30% over 2 min, and equilibrated at the initial conditions for 15 min. Products eluting at 22.5 and 31.2 min (UV absorbance at 280 nm; flow rate, 10 mL/min) were collected. The fractions were dried in vacuo and weighed. The identity of the product was confirmed by LC-ESI/MS and ^{1}H NMR. ^{1}H NMR spectra were recorded with a Varian 600 MHz NMR system (Varian Inc. Corp., Palo Alto, CA). Chemical shifts are expressed in ppm downfield shift from trimethylsilane (TMS) (δ scale). The synthesis of stable isotopically labeled surrogate standards was also performed on a small scale by the same method. The reaction products were purified using the LC-UV system.

Standard Solutions. ES-3′-C8-dG and ES-3′-N^2-dG were synthesized from 1′-acetoxy-ES and dG as described by Punt et al.[7] The yields

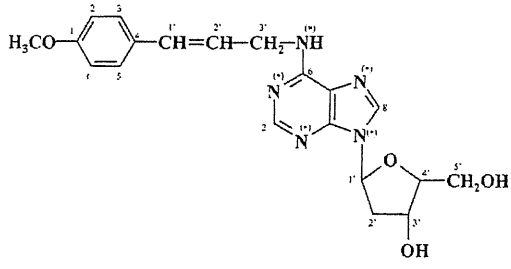

Figure 3. Chemical structure of ES-3′-N^6-dA adducts and the stable isotopically labeled compounds. The asterisk (*) indicates nitrogen [^{15}N]-labeling.

of ES-3′-C8-dG and ES-3′-N^2-dG were 63.4 (5.2%) and 103.5 mg (8.56%), respectively, in the reaction. The syntheses of [$^{15}N_5$]-ES-3′-8-dG, [$^{15}N_5$]-ES-3′-N^2-dG, and [$^{15}N_5$]-ES-3′-N^6-dA as stable isotopically labeled surrogate standards were also performed on a small scale by the same method. $^{15}N_5$-labeled ES-dG adducts including four isomers and ES-3′-N^6-dA were repeatedly purified using LC-UV system until 98% and over.

One millimolar solutions of ES-3′-C8-dG, ES-3′-N^2-dG, and ES-3′-N^6-dA were prepared in methanol and immediately diluted with methanol/HPLC grade water (50/50, v/v) to 10 μM (stock solution). Working solutions for calibration (0.01−10 nM for ES-3′-C8-dG, ES-3′-N^2-dG, and 0.003−10 nM for ES-3′- N^6-dA) were prepared by the addition of an adequate amount of surrogate standard and diluted with methanol/HPLC grade water (50/50, v/v) to appropriate concentrations.

LC-ESI/MS/MS Conditions. LC-ESI/MS/MS analyses were performed using a Quattoro Ultima (Micromass) coupled to a Hewlett Packard 1100 series (G1322A, degasser; G1312A, bin pump; G1316A, Colcom; G1329A, ALS; Agilent Technologies, Palo Alto, CA). The mass spectrometer was operated using an ESI source in the positive ion mode for multiple reaction monitoring (MRM). An aliquot (20 μL) of the sample was injected into a Mightysil C18-GP (2.0 mm × 150 mm, 5 μm; Kanto Chemical Co., Tokyo, Japan) maintained at 40 °C. Solvent A was 0.001% formic acid, and solvent B was 0.001% formic acid containing acetonitrile. The column was equilibrated with a mixture of solvent A/solvent B (75/25, v/v). The mobile phase consisted of a mixture of 0.001% formic acid/0.001% formic acid containing acetonitrile at an initial ratio of 75/25, employing a linear gradient to a final ratio of 30/70 (v/v) over 30 min, at a constant flow rate of 0.2 mL/min.

In the assay for ES-3′-N^2-dG and ES-3′-C8-dG, the precursor ion ([M + H]$^+$) was m/z 414, and the selected product ion [M + H − glycoside]$^+$ was m/z 298. Correspondingly, for [^{15}N]-labeled ES-3′-N^2-dG and ES-3′-C8-dG, the precursor ion was m/z 419, and the selected product ion was m/z 303. The cone voltage used was 18 V, and the collision energy was 10 eV. In the assay for ES-3′-N^6-dA, the precursor ion ([M + H]$^+$) was m/z 398, and the selected product ion [M + H − glycoside]$^+$ was m/z 282. Correspondingly, for [^{15}N]-labeled ES-3′-N^6-dA, the precursor ion was m/z 403, and the selected product ion was m/z 287. The cone voltage used was 12 V, and the collision energy was 18 eV. The source block temperature was 120 °C, and the desolvation temperature was 400 °C. The flow rate of the cone gas was set at 150 L/h, while that of the desolvation gas was set at 600 L/h. Under these conditions, the standard retention times were 11.8, 12.7, and 15.1 min for ES-3′-N^2-dG, ES-3′-C8-dG, and ES-3′-N^6-dA, respectively.

Recovery. The recovery was evaluated by calculating the mean of the response at each concentration. The spiked concentrations (low, middle, and high dose) of ES-3′-C8-dG, ES-3′-N^2-dG, and ES-3′-N^6-dA were determined from the concentrations of each compound in the liver DNA of control rats, using LC-ESI/MS/MS. A standard sample was

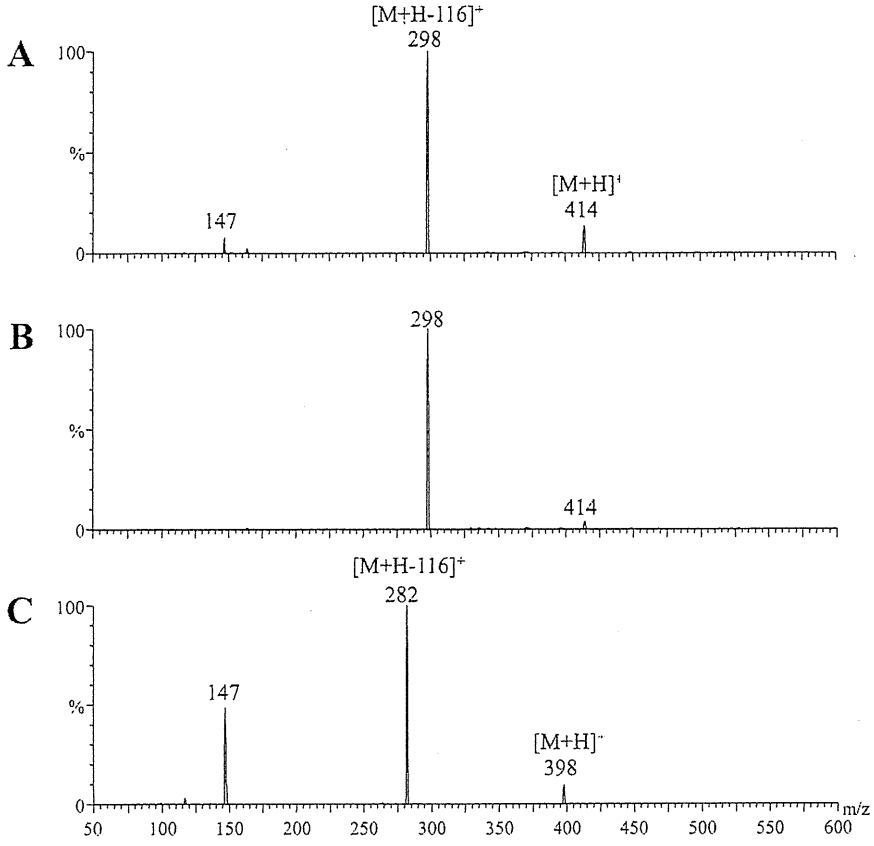

Figure 4. Product ion spectra of (A) ES-3′-C8-dG, (B) ES-3′-N^2-dG, and (C) ES-3′-N^6-dA. The cone voltages and collision energies were set at the optimum conditions for each compound in negative ion mode. LC-ESI/MS/MS conditions are described in the Materials and Methods.

added together with an adequate amount of surrogate standards to 20 mM sodium acetate buffer (pH 4.2) for DNA digestion so that the final concentration might be set to 0.05, 0.5, and 5 nM. The extracted DNA pellets of rat liver were redissolved in this buffer and digested according to the protocol. The sample was analyzed by LC-ESI/MS/MS, and the recovery rates were calculated.

Animal and Treatment. The protocol for this study was approved by the Animal Care and Utilization Committee of the National Institute of Health Sciences (Tokyo, Japan). Five week old male F344 rats were obtained from Japan SLC (Shizuoka, Japan). Ten rats were housed in polycarbonate cages (five rats per cage) with hardwood chips for bedding in conventional temperature (23 ± 2 °C), humidity (55 ± 5%), air change (12 times per hour), and lighting (12 h light/dark cycle) and were given free access to CRF-1 basal diet (Oriental Yeast Co., Ltd., Tokyo, Japan) and tap water. Groups of 10 rats were given ES by gavage in corn oil at 600 mg/kg bw per day, 5 days/week. All rats were killed at 4 weeks by exsanguination under ether anesthesia, and the livers were immediately removed and weighed. Samples were frozen with liquid nitrogen and stored at −80 °C until measurement of ES-specific DNA adducts.

DNA Isolation and Enzymatic Digestion. DNA extraction and digestion were performed according to the method of Nakae et al.[27] and our previous report.[28] The samples were homogenized with lysis buffer including commercial DNA isolation kit. The mixture was centrifuged at 10000*g* for 20 s at 4 °C. The deposit was dissolved in 200 μL of enzyme reaction buffer. After treatment with RNase and protease K, the DNA pellet was obtained by washing with 2-propanol and ethanol and centrifugation.

The dried DNA pellet was dissolved in surrogate standard containing 20 mM sodium acetate buffer, pH 4.8, and was incubated with 4 μL of nuclease P1 (2000 U/mL) at 70 °C for 15 min. Then, 20 μL of 1.0 M Tris-HCl buffer, pH 8.2, was added, and the sample was incubated with 4 μL of alkaline phosphatase (2500 U/mL) at 37 °C for 60 min. After the addition of 3.0 M sodium acetate buffer, pH 5.1, the digested DNA samples were used for adduct analysis and base analysis. Then, 50 μL of the digested sample for dG and dA analysis was passed through 100000 NMWL filter (Millipore, Bedford, MA) and injected into the LC-UV. One hundred microliters of digested sample for adduct analysis was diluted with an equal volume of methanol and injected into the LC-ESI/MS/MS.

LC-UV Analysis for dG and dA. dG and dA were determined by an LC-UV system (Jasco Co.: PU-980 Intelligent HPLC Pump, AS-950-10 Intelligent Sampler, CO-1560 Intelligent Column Thermostat, MD-1515 Multiwavelength Detector, Tokyo, Japan). Two milliliters of sample was injected directly on to a reversed phase C18 column (Ultrasphere ODS, 4.6 mm × 250 mm, 5 μm, Beckman Coulter, Inc.) maintained at 40 °C. Solvent A was 0.01% formic acid containing water, and solvent B was 0.01% formic acid containing methanol. The column was equilibrated with a mixture of solvent A/solvent B (98/2, v/v). The compounds were eluted at a flow rate of 1.0 mL/min. A linear gradient was applied from 2 to 10% methanol over 20 min, kept at 10% for 5 min, lowered to 2% over 2 min, and equilibrated at these initial conditions for 15 min. The wavelength of the UV detector was set at 280 nm for the detection of dG and dA.

RESULTS

Identification of Luc-N^6-dA. The reaction mixtures for 1′-acetoxy-ES with/without dA were separated by LC-PDA-ESI/MS.

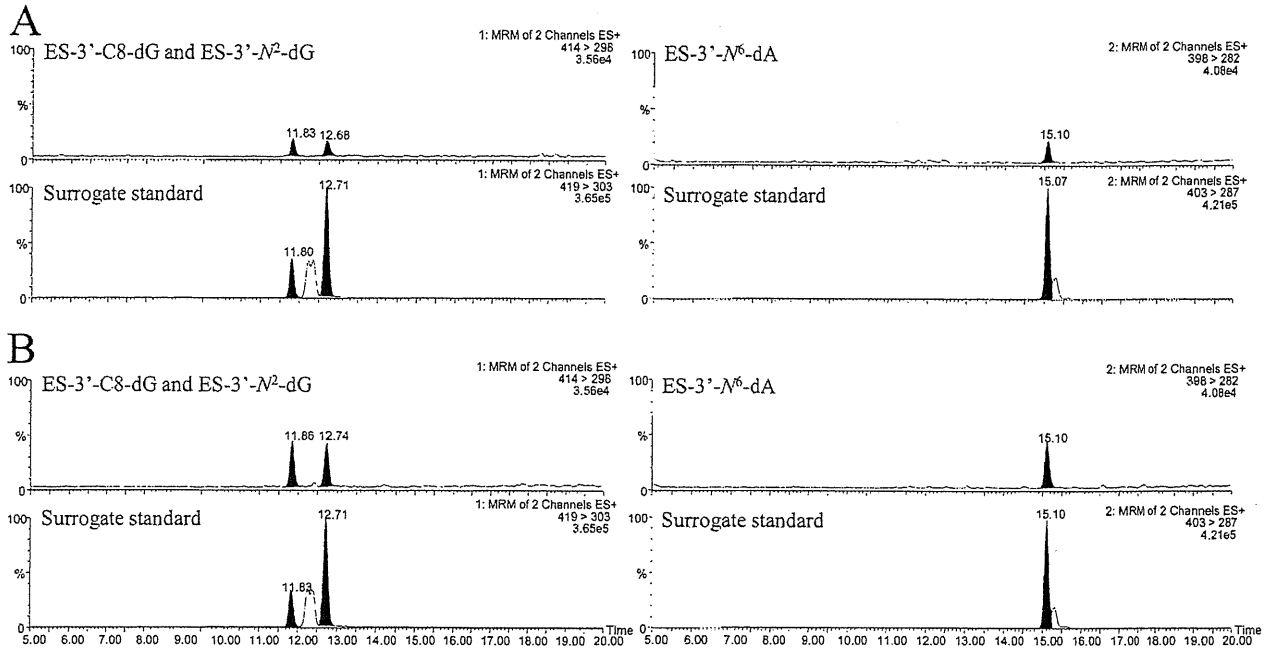

Figure 5. MRM chromatograms of LOD (A) and LOQ (B) levels of ES-3′-C8-dG, ES-3′-N^2-dG, and ES-3′-N^6-dA adducts and each surrogate standard from extracted DNA samples.

Table 2. Recoveries of ES-3′-C8-dG, ES-3′-N^2-dG, and ES-3′-N^6-dA Adducts in Rat Liver Samples

compounds	added (pmol/L)	concentration (pmol/L)	recovery (%)	RSD (%)
ES-3′-C8-dG (n = 5)	50	50.0 ± 2.3	98.0 ± 4.6	4.7
	500	501.1 ± 26.5	100.3 ± 5.3	5.3
	5000	4938.8 ± 135.5	98.8 ± 2.7	2.7
ES-3′-N^2-dG (n = 5)	50	50.6 ± 3.7	101.3 ± 7.5	7.4
	500	497.2 ± 18.6	99.4 ± 3.7	3.7
	5000	4981.2 ± 79.2	99.6 ± 1.6	1.6
ES-3′-N^6-dA (n = 5)	50	51.7 ± 0.77	103.5 ± 1.5	1.5
	500	509.9 ± 7.29	102.0 ± 1.5	1.4
	5000	4988.0 ± 109.8	99.8 ± 2.2	2.2

Typical LC-PDA chromatograms are shown in Figure 1A,B. Two unknown peaks were observed in the PDA chromatogram (280 nm) after the reaction of 1′-acetoxy-ES with dA (Figure1B). Simultaneously, mass spectra and UV−vis absorption spectra were obtained by ESI/MS (cone voltage 20, 40, and 60 V) and PDA. MS spectra of all unknown peaks were analyzed according to the ES and dA structure, and then, two peaks were analyzed in the chromatograms. One of the two peaks (peak 1) was observed at 22.1 min in the chromatogram of dA reaction (Figure 1B). The UV−vis absorption spectrum of peak 1 had λ_{max} at 260 nm. In the mass spectra of peak 1 when the cone voltage was set at 20 V (Figure 2A), the precursor ion ($[M + H]^+$, m/z 398) and product ion (m/z 282), corresponding to an ES-adenine adduct following glycoside bond cleavage, were clearly observed. A product ion (m/z 147) corresponding to 2-allyl-4-mthoxybenzene structure was observed in the mass spectra at 40 and 60 V (Figure 2B,C). The other peak (peak 2) was observed at 22.4 min in the chromatogram for the reaction of 1′-acetoxy-ES and dA (Figure 1B). The UV−vis absorption spectrum was virtually identical to peak 1 and also had at λ_{max} at 260. In the mass spectra of peak 2 when the cone voltage was set at 20 and 40 V (Figure 2D,E), the precursor ion ($[M + H]^+$, m/z 398) and product ion (m/z 282), corresponding to ES-adenine adduct following glycoside bond cleavage, were clearly observed. A product ion (m/z 147) corresponding to 2-allyl-4-mthoxybenzene structure was also observed in the mass spectra of 40 and 60 V (Figure 2E,F).

1′-Acetoxy-ES was used as an electrophilic synthon in large scale synthesis to identify the chemical structures of peaks 1 and 2 from dA, respectively. These adducts were synthesized repeatedly by reaction with each base until the quantity was sufficient for ^{1}H NMR after HPLC-UV chromatography. However, peak 2 could not be collected in sufficient amounts for structural analysis. ^{1}H NMR chemical sifts of peak 1 redissolved in DMSO-d_6 are shown in Table 1. On the basis of these data, we judged that peak 1 was ES-3′-N^6-dA. Chemical structures of ES-3′-N^6-dA and stable isotopically labeled compound as a surrogate standard for LC-ESI/MS/MS analysis are shown in Figure 3.

Optimal Conditions for LC-MS/MS Detection. Figure 4 shows the product ion spectra for ES-3′-C8-dG, ES-3′-N^2-dG,

dx.doi.org/10.1021/tx100410y |Chem. Res. Toxicol. 2011, 24, 532–541

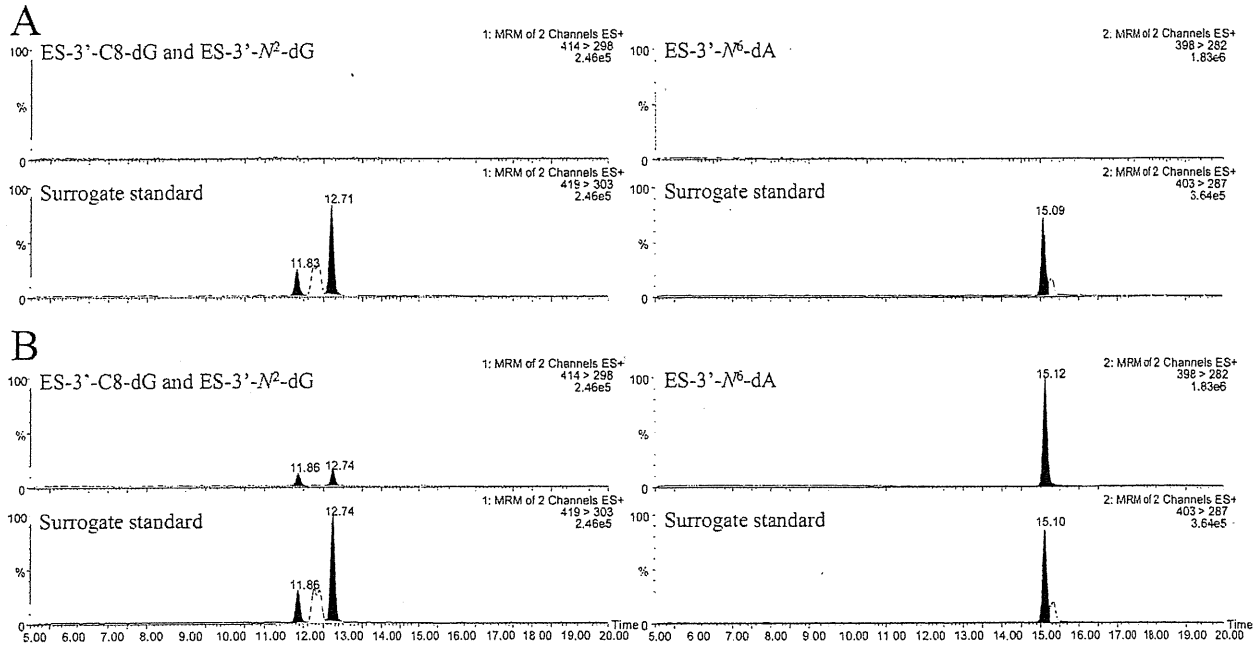

Figure 6. MRM chromatograms of ES-3′-C8-dG, ES-3′-N^2-dG, and ES-3′-N^6-dA adducts and each surrogate standard in rat liver DNA samples. (A) Liver from rat administrated with vehicle as a control group. (B) Liver from rat orally administrated with 600 mg/kg ES for 4 weeks.

Table 3. LC-MS/MS Analysis of Liver DNA Samples Obtained from Rats Treated with 600 mg/kg bw ES for up to 4 Weeks

group	sample no.	ES-3′-C8-dG/10^6dG	ES-3′-N^2-dG/10^6dG	ES-3′-N^6-dA/10^6dA
control	1	ND[a]	ND	ND
	2	ND	ND	ND
	3	ND	ND	ND
	4	ND	ND	ND
	5	ND	ND	ND
	average			
ES (600 mg/kg)	6	3.02	4.16	18.96
	7	3.53	4.28	20.05
	8	3.42	4.37	21.22
	9	4.12	6.18	22.89
	10	3.33	5.07	20.47
	average	3.48 ± 0.40	4.81 ± 0.84	20.47 ± 1.61

[a] ND, not detected.

and ES-3′-N^6-dA. The mass spectrometer equipped with an ESI source using a crossflow counter electrode was run in positive ion mode to detect MRM of the transitions 414 > 298, 414 > 298, and 398 >282, respectively.

The crucial parameters affecting LC-ESI/MS/MS, namely, cone voltage, collision energy, and mobile phase, were investigated. To establish the optimum cone voltage and collision energy for the detection of these adducts, the signals at m/z 414 and 419 precursor ions versus cone voltage were investigated, respectively. The optimal cone voltages were 18, 18, and 12 V in the negative ion mode for ES-3′-C8-dG, ES-3′-N^2-dG, and ES-3′-N^6-dA standard solutions, respectively. Then, the m/z 298 and 282 product ion signals versus collision energy were investigated, respectively. The optimal collision energies were 10, 10, and 18 eV for ES-3′-C8-dG, ES-3′-N^2-dG, and ES-3′-N^6-dA standard solutions, respectively. The ionization of the samples at the LC-MS interface was affected by the mobile phase; hence, a mobile phase containing a volatile acid or salt was generally used. In this study, the responses were measured using 0−0.1% formic acid in water−acetonitrile (v/v) as the mobile phase. The responses of ES-3′-C8-dG, ES-3′-N^2-dG, and ES-3′-N^6-dA were increased by the addition of formic acid to the mobile phase. The increase in response reached a maximum and leveled off when 0.001% formic acid was added.

Validation of LC-MS/MS. The calculated instrument detection limit (IDL) of ES-3′-C8-dG, ES-3′-N^2-dG, and ES-3′-N^6-dA of the standard solutions was 3.0, 3.0, and 1.0 pM, respectively, for LC-MS/MS detection at the ratio of the compound's signal to the background signal (S/N) of 3. In addition, the instrument quantification limit (IQL) was calculated when S/N = 10 was 10, 10, and 3.0 pM, respectively. The limit of detection (LOD) and limit of quantification (LOQ) in the real sample were the same as IDL and

Table 4. Interday Precision for the Determination of ES-3′-C8-dG, ES-3′-N^2-dG, and ES-3′-N^6-dA Adduct Levels in the Rat Liver DNA Samples on Five Different Days Using LC-MS/MS

	repeat analysis of ES-3′-8- dG adduct (nM)						
sample no.	day 1	day 2	day 3	day 4	day 5	mean (nmol/L)	RSD (%)
6	0.510	0.518	0.491	0.506	0.509	0.507 ± 0.010	1.96
7	0.431	0.443	0.450	0.432	0.459	0.443 ± 0.012	2.68
8	0.462	0.470	0.482	0.483	0.445	0.468 ± 0.016	3.39
9	0.474	0.490	0.480	0.458	0.476	0.476 ± 0.011	2.39
10	0.484	0.483	0.483	0.511	0.447	0.482 ± 0.023	4.74
	repeat analysis of ES-3′-N^2-dG adduct (nM)						
sample no.	day 1	day 2	day 3	day 4	day 5	mean (nmol/L)	RSD (%)
6	0.701	0.711	0.733	0.703	0.727	0.715 ± 0.014	1.97
7	0.522	0.597	0.597	0.586	0.546	0.569 ± 0.034	5.91
8	0.590	0.626	0.608	0.638	0.605	0.613 ± 0.019	3.06
9	0.711	0.706	0.705	0.678	0.661	0.692 ± 0.022	3.15
10	0.737	0.676	0.717	0.706	0.718	0.711 ± 0.022	3.13
	repeat analysis of ES-3′-N^6-dA adduct (nM)						
sample no.	day 1	day 2	day 3	day 4	day 5	mean (nmol/L)	RSD (%)
6	3.100	2.967	3.098	3.044	2.949	3.032 ± 0.071	2.36
7	2.286	2.333	2.236	2.339	2.250	2.289 ± 0.047	2.04
8	2.699	2.617	2.738	2.797	2.766	2.723 ± 0.069	2.55
9	2.444	2.455	2.546	2.506	2.526	2.495 ± 0.044	1.77
10	2.736	2.735	2.846	2.880	2.830	2.805 ± 0.066	2.36

IQL, respectively. The peak area ratio with respect to each surrogate standard was plotted, and the response was found to be linear (ES-3′-C8-dG, $y = 1.9707x - 0.0096$ and $y = 2.0318x - 0.0989$; ES-3′-N^2-dG, $y = 0.6359x + 0.0048$ and $y = 0.6336x - 0.0263$; and ES-3′-N^6-dA, $y = 1.8567x + 0.012$ and $y = 1.8205x + 0.065$) over the calibration range, from LOQ to 1.0 nM (low range) and from 0.1 to 10 nM (high range), with a correlation coefficient (r) of over 0.999. The average retention times of ES-3′-C8-dG, ES-3′-N^2-dG, and ES-3′-N^6-dA standards were 11.8 (RSD = 0.08%, n = 5), 12.7 (RSD = 0.12%, n = 5), and 15.1 min (RSD = 0.06%, n = 5), respectively. MRM chromatograms of the mixture of three adduct and their corresponding surrogate standards in 50% methanol at LOD and LOQ levels are shown in Figure 5.

As shown in Table 2, the average recoveries of ES-3′-C8-dG, ES-3′-N^2-dG, and ES-3′-N^6-dA from DNA sample in the livers of nontreated rats were 99.0, 100.1, and 101.7% for each adduct.

Analysis of ES-N^2-dG, C8-dG, and N^6-dA in the Livers DNA Extracted from Rats Treated with ES. The potential formation of ES adducts in livers of rats exposed to ES was assessed using the isotope dilution LC-ESI/MS/MS method. Typical selected ion recording (SIR) chromatograms are shown in Figure 6. No peaks indicative of ES-3′-C8-dG, ES-3′-N^2-dG, and ES-3′-N^6-dA were observed in liver DNA extracted from control rats. In contrast, ES-3′-C8-dG, ES-3′-N^2-dG, and ES-3′-N^6-dA were detected at 11.8, 12.7, and 15.1 min in the liver DNA MRM chromatograms extracted from rats treated with 600 mg/kg ES for up to 4 weeks, respectively. Quantitative data are summarized in Table 3. The ES-3′-C8-dG, ES-3′-N^2-dG/10^6dG, and ES-3′-N^6-dA/10^6dA ratios were 3.5 ± 0.4, 4.8 ± 0.8, and 20.5 ± 1.6, respectively. The interday sample variation of ES-3′-C8-dG, ES-3′-N^2-dG, and ES-3′-N^6-dA adduct levels analyzed on different days resulted in an average coefficient of variation (CV) of 3.0, 3.4, and 2.2% for different samples that were analyzed (Table 4). All of these adducts were not detected in the control group.

DISCUSSION

Phillips et al. have suggested the chemical structure of four ES-specific DNA adducts, ES-3′-N^2-dG, ES-3′-C8-dG, ES-1′-N^2-dG, and ES-3′-N^6-dA, using radio isotope-labeled nucleosides. The formation of these adducts in mouse liver treated with [^{14}C]-labeled ES was demonstrated by radioactive detection after HPLC fractionation.[8] Subsequently, LC-MS analysis by Punt et al. demonstrated the formation of three ES-dG adducts, ES-3′-N^2-dG, ES-3′-C8-dG, and ES-1′-N^2-dG, after in vitro nucleoside reaction.[7] However, the existence of the dA adduct reported previously and its chemical structure have not been confirmed using MS technique. In the present study, we examine dA adduct formation using LC-ESI/MS by taking advantage of reactive carbocation formation generated by acetylation of ES proposed by Punt et al.[7] In the reaction of dA with 1′-acetoxy-ES, two peaks including ions characteristic for the ES-dA adduct were observed by total ion chromatography. Subsequently, ^{1}H NMR analysis of large-scale synthesized and HPLC purified samples led to the conclusion that the major adduct was ES-3′-N^6-dA, in line with the previous report.[8] Although a minor and unknown ES-dA adduct was also found, its precise chemical structure could not be elucidated due to the low yield.

dx.doi.org/10.1021/tx100410y |Chem. Res. Toxicol. 2011, 24, 532–541

ES has been reported to have genotoxicity and carcinogenicity in the livers of mice of both sexes.[2] ES treatment at a dose of 600 mg/kg by gavage for 16 weeks induced significant developments of glutathione S-transferase placenta form (GST-P) foci in the liver of rats (unpublished data). To examine the precise quantity of ES-specific adducts in ES-hepatocarcinogenesis, we used interim samples (4 weeks) for the carcinogenicity study mentioned above. On the basis of previous reports, we attempted to detect ES-3′-N^2-dG, ES-3′-C8-dG, and ES-3′-N^6-dA. Because appropriate sample preparations and a highly sensitive analytical method are necessary to detect modified DNA bases in genomic DNA, we developed a new analytical method by an isotope dilution LC-ESI/MS/MS method using SIR. ^{32}P-postlabeling analysis without internal standards for identifying the products neither provides structural characterization of adducts nor has sufficient selectivities. In addition, this assay requires radioactive γ-^{32}P-labeled ATP in the analytical process, which raises the necessity of rigorous handling. The LC-MS/MS technique using stable isotope adducts as internal standards achieves accurate quantification of DNA adducts along with structural characterization. The LOQs of ES-3′-N^2-dG, ES-3′-C8-dG, and ES-3′-N^6-dA in our method were determined to be 2−5 adducts/10^8 unmodified dG or dA bases from a 150 mg liver sample. In addition, the high recoveries of these adducts in the wide range from LOQ level indicated that our new method enables precise adduct determination with the use of surrogate standards and is applicable to the detection of these compounds in animal tissue samples. As a result, our method was able to quantify these three adducts in liver DNA of rats treated with 600 mg/kg ES for 4 weeks, and we observed that the ES-3′-N^6-dA adduct is predominant. Phillips et al. have suggested that ES-3′-N^2-dG was a major adduct in the livers of mice treated with single dose of 1′-hydroxy-ES (12 μmol/mouse), a metabolite of ES. Considering that the present experiment was performed under carcinogenic conditions, it is highly probable that the status of DNA adduct formation observed in the present study may be reflected in the ES carcinogenesis. The modification at the N^6-position of dA has been reported following treatment with other potent mutagens including aristolochic acid,[22,23] polyaromatic hydrocarbon, benzo[*c*]phenanthrene,[29,30] and 5,6-dimathylchrysene.[31] It is likely that the formation of various types of chemical-specific base modifications is dependent on accessibility of the chemical (or the proximate form) to the reactive amino group between dG and dA in the DNA helical structure.[32] Those mutagens predominantly induce AT-TA transversion and AT-GC transition mutations.[25,33,34] Therefore, our unpublished data that the AT-GC transition mutation was predominant in ES-treated rat livers allow us to hypothesize that N^6-dA adducts might play a key role in ES mutagenicity. Thus, information regarding the precise concentrations of ES-specific DNA adducts discovered in the present study would be very helpful for further research on ES hepatocarcinogenesis.

Minor adducts of dG (ES-1′-N^2-dG) and dA (not identified) were hardly detected in in vivo samples even though such adducts are detectable in the reaction of 1′-acetoxy-ES with deoxynucleoside.[7] Dissociation of the ester group from an ester of 1-hydroxy-ES generates an electrophilic ion in which the positive charge may reside on the double bond between the 2-, 3- and 1-, 2-positions on the allyl chain. Nucleophilic attack by the purine bases of DNA at the 1′-position of ES would account for ES-1′-N^2-dG formation, while attack at the 3′-position would account for ES-3′-N^2-dG. Because dG modification at the 3′-position of ES far from the benzene ring is predominant both in vivo and in vitro, it is conceivable that the priority of these reactions is determined by steric hindrance between DNA bases and ES. The suggestion that unknown minor dA adducts also might result from modification at the 1′-position of ES is in line with this hypothesis. Therefore, the fact that genomic DNA possesses more steric hindrance than nucleosides might explain the lack of detection of these minor adducts in vivo.

In conclusion, dA modified by ES was determined to be EG-3′-N^6-dA as the major adduct. ES-3′-N^2-dG, ES-3′-C8-dG, and ES-3′-N^6-dA adducts can be identified and quantified by this new method, which may prove useful in other related studies.

AUTHOR INFORMATION

Corresponding Author

*Tel: +81-3-3700-9819. Fax: +81-3-3700-1425. E-mail: y-ishii@nihs.go.jp.

ABBREVIATIONS

ES, estragole; dG, deoxyguanosine; dA, deoxyadenosine; LC, liquid chromatography; ESI, electron spray ionization; MS, mass spectrometry; NMR, nuclear magnetic resonance; MS/MS, tandem mass spectrometry; SIR, selected ion recording; LOQ, limit of quantification; SULT, sulfotransferase; THF, tetrahydrofuran; DMSO, dimethylsulfoxide; DMF, dimethylformamide; TMS, trimethylsilane; MRM, multiple reaction monitoring; PDA, photodiode array; IDL, instrument detection limit; IQL, instrument quantification limit; LOD, limit of detection; GST-P, glutathione S-transferase placenta form.

REFERENCES

(1) Smith, R. L., Adams, T. B., Doull, J., Feron, V. J., Goodman, J. I., Marnett, L. J., Portoghese, P. S., Waddell, W. J., Wagner, B. M., and Rogers, A. E. (2002) Safety assessment of allylalkoxybenzene derivatives used as flavouring substances-Methyl eugenol and estragole. *Food Chem. Toxicol. 40*, 851–870.

(2) Drinkwater, N. R., Miller, E. C., Miller, J. A., and Pilot, H. C. (1976) Hepatocarcinogenicity of estragole (1-allyl-4-methoxybenzene) and 1′-hydroxyestragole in the mouse and mutagenicity of 1′-aceotyestragole in bacteria. *J. Natl. Cancer Inst. 57*, 1323–1331.

(3) Miller, E. C., Swanson, A. B., Phillips, D. H., Fletcher, T. L., Liem, A., and Miller, J. A. (1983) Structure-activity studies of the carcinogenicities in the mouse and rat of some naturally occurring and synthetic alkenylbenzene derivatives related to safrole and estragole. *Cancer Res. 43*, 1124–1134.

(4) Wiseman, R. W., Miller, E. C., Miller, J. A., and Liem, A. (1987) Structure-activity studies of the hepatocarcinogenicities of alkenylbenzene derivatives related to estragole and safrole on administration to preweanling male C57BL/6J x C3H/HeJ F_1 mice. *Cancer Res. 47*, 2275–2283.

(5) Jeurissen, S. M., Punt, A., Boersma, M. G., Bogaards, J. J. P., Fiamegos, Y. C., Schilter, B., Van Bladeren, P. J., Cnubben, N. H. P., and Rietjens, I. M. C. M. (2007) Human cytochrome P450 enzyme specificity for the bioactivation of estragole and related alkenylbenzenes. *Chem. Res. Toxicol. 20*, 798–806.

(6) Fennell, T. R., Wiseman, R. W., Miller, J. A., and Miller, E. C. (1985) Major role of hepatic sulfotransferase activity in the metabolic activation, DNA adduct formation, and carcinogenicity of 1′-hydroxy-2′3′-dehydroestragole in infant male C57BL/6J x C3H/HeJ F1 mice. *Cancer Res. 45*, 5310–5320.

(7) Punt, A., Delatour, T., Scholz, G., Schilter, B., van Bladeren, P. J., and Rietjens, I. M. (2007) Tandem mass spectrometry analysis of N^2-(trans-isoestragol-3′-yl)-2′-deoxyguanosine as a strategy to study

species differences in sulfotransferase conversion of the proximate carcinogen 1′-hydroxyestragole. *Chem. Res. Toxicol. 20*, 991–998.

(8) Phillips, D. H., Reddy, M. V., Miller, E. C., and Adams, B. (1981) Structures of the DNA adducts formed in mouse liver after administration of the proximate hepatocarcinogen 1′-hydroxyestragole. *Cancer Res. 41*, 176–186.

(9) Phillips, D. H., Reddy, M. V., and Randerath, K. (1984) ^{32}P-post-labelling analysis of DNA adducts formed in the livers of animals treated with safrole, estragole and other naturally-occurring alkenylbenzens II. Newborn male B6C3F1 mice. *Carcinogenesis 5*, 1623–1628.

(10) Rnaderathe, K., Haglund, R. E., Phillips, D. H., and Reddy, M. V. (1984) ^{32}P-post-labelling analysis of DNA adducts formed in the livers of animals treated with safrole, estragole and other naturally-occurring alkenylbenzenes. I. Adult female CD-1 mice. *Carcinogenesis 5*, 1613–1622.

(11) Wiseman, R. W., Fennell, T. R., Miller, J. A., and Miller, E. C. (1985) Further characterization of the DNA adducts formed by electrophilic esters of the hepatocarcinogens 1′-hydroxysafrole and 1′-hydroxyestragole in vitro and in mouse liver in vivo, including new adducts at C-8 and N-7 of guanine residues. *Cancer Res. 45*, 3096–3105.

(12) Prakash, A. S., Tran, H. P., Peng, C., Koyalamudi, S. R., and Dameron, C. T. (2000) Kinetics of DNA alkylation, depurination and hydrolysis of anti diol epoxide of benzo(a)pyrene and the effect of cadmium on DNA alkylation. *Chem.-Biol. Interact. 125*, 133–150.

(13) Moustacchi, E. (2000) DNA damage and repair: Consequences on dose-responses. *Mutat. Res. 464*, 35–40.

(14) Choi, J. Y., and Guengerich, F. P. (2005) Adduct size limits efficient and error-free bypass across bulky N2-guanine DNA lesions by human DNA polymerase eta. *J. Mol. Biol. 352*, 72–90.

(15) Wei, D., Maher, V. M., and McCormick, J. J. (1996) Site-specific excision repair of 1-nitrosopyrene-induced DNA adducts at the nucleotide level in the HPRT gene of human fibroblasts: Effect of adduct conformation on the pattern of site-specific repair. *Mol. Cell. Biol. 16*, 3714–3719.

(16) Singh, R., Gaskell, M., Le Pla, R. C., Kaur, B., Azim-Araghi, A., Roach, J., Koukouves, G., Souliotis, V. L., Kyrtopoulos, S. A., and Farmer, P. B. (2006) Detection and quantification of benzo[a]pyrene-derived DNA adducts in mouse liver by liquid chromatography-tandem mass spectrometry: comparison with 32P-postlabeling. *Chem. Res. Toxicol. 19*, 868–878.

(17) Pfau, W., Brockstedt, U., Söhren, K. D., and Marquardt, H. (1994) 32P-post-labelling analysis of DNA adducts formed by food-derived heterocyclic amines: Evidence for incomplete hydrolysis and a procedure for adduct pattern simplification. *Carcinogenesis 15*, 877–882.

(18) Lyle, T. A., Royer, R. E., Daub, G. H., and Vander Jagt, D. L. (1980) Reactivity-selectivity properties of reactions of carcinogenic electrophiles and nucleosides: Influence of pH on site selectivity. *Chem.-Biol. Interact. 29*, 197–207.

(19) Yuan, B., Cao, H., Jiang, Y., Hong, H., and Wang, Y. (2008) Efficient and accurate bypass of N2-(1-carboxyethyl)-2′-deoxyguanosine by DinB DNA polymerase in vitro and in vivo. *Proc. Natl. Acad. Sci. U.S.A. 105*, 8679–8684.

(20) Xu, P., Oum, L., Geacintov, N. E., and Broyde, S. (2008) Nucleotide selectivity opposite a benzo[a]pyrene-derived N2-dG adduct in a Y-family DNA polymerase: A 5′-slippage mechanism. *Biochemistry 47*, 2701–2709.

(21) Stover, J. S., Chowdhury, G., Zang, H., Guengerich, F. P., and Rizzo, C. J. (2006) Translesion synthesis past the C8- and N2-deoxyguanosine adducts of the dietary mutagen 2-Amino-3-methylimidazo[4,5-f]quinoline in the Narl recognition sequence by prokaryotic DNA polymerases. *Chem. Res. Toxicol. 19*, 1506–1517.

(22) Chan, W., Yue, H., Poon, W. T., Chan, Y. W., Schmitz, O. J., Kwong, D. W., Wong, R. N., and Cai, Z. (2008) Quantification of aristolochic acid-derived DNA adducts in rat kidney and liver by using liquid chromatography-electrospray ionization mass spectrometry. *Mutat. Res. 646*, 17–24.

(23) Grollman, A. P., Shibutani, S., Moriya, M., Miller, F., Wu, L., Moll, U., Suzuki, N., Fernandes, A., Rosenquist, T., Medverec, Z., Jakovina, K., Brdar, B., Slade, N., Turesky, R. J., Goodenough, A. K., Rieger, R., Vukelić, M., and Jalaković, B. (2007) Aristolochic acid and the etiology of endemic (Balkan) nephropathy. *Proc. Natl. Acad. Sci. U.S.A. 104*, 12129–12134.

(24) Kim, S. J., Jajoo, H. K., Kim, H. Y., Zhou, L., Horton, P., Harris, C. M., and Harris, T. M. (1995) An efficient route to N^6 deoxyadenosine adducts of diol epoxides of carcinogenic polycyclic aromatic hydrocarbons. *Bioorg. Med. Chem. 3*, 811–822.

(25) Schmeiser, H. H., Scherf, H. R., and Wiessler, M. (1991) Activating mutations at codon 61 of the c-Ha-ras gene in thin-tissue sections of tumors induced by aristolochic acid in rats and mice. *Cancer Lett. 59*, 139–143.

(26) Schmeiser, H. H., Janssen, J. W., Lyons, J., Scherf, H. R., Pfau, W., Buchmann, A., Bartram, C. R., and Wiessler, M. (1990) Aristolochic acid activates ras genes in rat tumors at deoxyadenosine residues. *Cancer Res. 50*, 5464–5469.

(27) Nakae, D., Mizumoto, E., Kobayashi, E., Noguchi, O., and Konishi, Y. (1995) Improved genomic/nuclear DNA extraction for 8-hydroxydeoxyguanosine analysis of small amounts of rat liver tissue. *Cancer Lett. 97*, 233–239.

(28) Ishii, Y., Okamura, T., Inoue, T., Fukuhara, K., Umemura, T., and Nishikawa, A. (2010) Chemical structure determination of DNA bases modified by active metabolites of lucidin-3-O-primeveroside. *Chem. Res. Toxicol. 23*, 134–141.

(29) Yakovleva, L., Handy, C. J., Sayer, J. M., Pirrung, M., Jerina, D. M., and Shuman, S. (2004) Benzo[c]phenanthrene adducts and nogalamycin inhibit DNA transesterification by vaccinia topoisomerase. *J. Biol. Chem. 279*, 23335–23342.

(30) Ponten, I., Sayer, J. M., Pilcher, A. S., Yagi, H., Kumar, S., Jerina, D. M., and Dipple, A. (1999) Sequence context effects on mutational properties of cis-opened benzo[c]phenanthrene diol epoxide-deoxyadenosine adducts in site-specific mutation studies. *Biochemistry 38*, 1144–1152.

(31) Misra, B., Amin, S., and Hecht, S. S. (1992) Dimethylchrysene diol epoxides: Mutagenicity in Salmonella typhimurium, tumorigenicity in newborn mice, and reactivity with deoxyadenosine in DNA. *Chem. Res. Toxicol. 5*, 248–254.

(32) Blake, R. D. (2005) *Informational Biopolymers of Genes and Gene Expression*, p 290, University Science Books, CA.

(33) Page, J. E., Szeliga, J., Amin, S., Hecht, S. S., and Dipple, A. (1995) Mutational spectra for 5,6-dimethylchrysene 1,2-dihydrodiol 3,4-epoxides in the supF gene of pSP189. *Chem. Res. Toxicol. 8*, 143–137.

(34) Schmeiser, H. H., Janssen, J. W., Lyons, J., Scherf, H. R., Pfau, W., Buchmann, A., Bartram, C. R., and Wiessler, M. (1990) Aristolochic acid activates ras genes in rat tumors at deoxyadenosine residues. *Cancer Res. 50*, 5464–5469.